

Coupled Chemical Reactions: Effects of Electric Field, Diffusion and Boundary Control

Shixin Xu* Robert Eisenberg[†] Zilong Song[‡] Huaxiong Huang[§]

Abstract

Chemical reactions involve the movement of charges, and this work presents a mathematical model for describing chemical reactions in electrolytes. The model is developed using an energy variational method that aligns with classical thermodynamics principles. It encompasses both electrostatics and chemical reactions within consistently defined energetic and dissipative functionals. Furthermore, the energy variation method is extended to account for open systems that involve the input and output of charge and mass. Such open systems have the capability to convert one form of input energy into another form of output energy. In particular, a two-domain model is developed to study a reaction system with self-regulation and internal switching, which plays a vital role in the electron transport chain of mitochondria responsible for ATP generation—a crucial process for sustaining life. Simulations are conducted to explore the influence of electric potential on reaction rates and switching dynamics within the two-domain system. It shows that the electric potential inhibits the oxidation reaction while accelerating the reduction reaction.

Keywords— Open system, Mass action, Electrochemistry

1 Introduction

Theories for chemical reactions based on the law of mass actions often ignore electric effects [11, 27], even though the reactants, catalysts and enzymes of chemistry and biology depend on charge interactions for much of their function [52, 73, 15]. Recently, mathematical models have been developed in the electrochemical tradition [25, 2, 3, 56, 9], some using variational principles [63, 62]. Here, we extend this work by proposing a general thermodynamics-consistent framework for electrochemical reactions both in the bulk and on the interface in biological systems. Specifically, we investigate the electric effects on the rate of chemical reactions using several reduced (‘toy’) models that show interesting dynamics and interactions between diffusion, reaction, and electric fields of ionic solutions.

Various consistent frameworks have been developed for nonequilibrium systems based on the second law of thermodynamics and Onsager’s linear response theory. Onsager’s variational principle, which was first proposed in [43, 44] and later generalized by Edwards [20], Doi [19], and Qian [46], is a popular

*Zu Chongzhi Center for Mathematics and Computational Sciences, Duke Kunshan University, 8 Duke Ave, Kunshan, Jiangsu, China.

[†]Department of Applied Mathematics, Illinois Institute of Technology, Chicago, IL, 60616, USA; Department of Physiology and Biophysics, Rush University, Chicago, IL, 60612, USA.

[‡]Math and Statistics Department, Utah State University, Old Main Hill Logan, UT 84322.

[§]Corresponding author, Research Center for Mathematics, Advanced Institute of Natural Sciences, Beijing Normal University, Zhuhai, Guangdong, 519088, China; Guangdong Provincial Key Laboratory of Interdisciplinary Research and Application for Data Science, BNU-HKBU United International College, Zhuhai, Guangdong, 519088, China; Laboratory of Mathematics and Complex Systems, MOE, Beijing Normal University, 100875 Beijing, China; Department of Mathematics and Statistics York University, Toronto, ON, M3J 1P3, Canada (hhuang@uic.edu.cn).

approach to irreversible systems. It is based on the maximum dissipation principle proposed by Lord Rayleigh [54] motivated by the analysis of uncharged systems. The principle states that for a system described by variables $\alpha_1, \dots, \alpha_n$ that describe the displacement from thermodynamic equilibrium with the (corresponding) rates $\dot{\alpha}_1, \dots, \dot{\alpha}_n$, and with free energy $F(\alpha_1, \dots, \alpha_n)$, the thermodynamic flux $\dot{\alpha}_i$ follows the dynamic path that minimizes the Rayleigh function. This function is the sum of the dissipation function Φ and the rate of the change of the free energy \dot{F} in an isothermal system. [60] provide a more detailed review. In order to include the fluid kinetic energy [24] for fluid equations, Wang et al. [61, 71] proposed the Generalized Onsager principle (GOP) for both reversible and irreversible processes.

Energetic Variational Approach (EnVarA) is another powerful tool proposed by Liu et al. [48, 21, 67]. The general framework of EnVarA is a combination of statistical physics and nonlinear thermodynamics. All the physics are integrated into the definitions of total energy E and dissipation functional Δ . The Least action principle [23] yields the conservative force F_{con} by taking the variation of the action functional with respect to the flow map in the Lagrange frame of reference. The Maximum principle [43, 44] yields dissipative force F_{dis} by taking the variation of the rate function. The final equation of momentum is achieved by balancing these two forces balance $F_{con} = F_{dis}$. A more detailed review can be found in [62].

Based on the consideration of the second law of thermodynamics, in particular, the requirement that the rate of energy dissipation needs to be non-positive, Ren et al. [47, 75, 74] proposed a more straightforward method built on a concept in [29]. First, the energy functional E is defined according to different physical fields. Based on the laws of conservation, the kinematic assumptions are listed with unknown terms like fluxes and stresses. By taking the time derivative of the total energy $\frac{dE}{dt}$, those unknowns could be described so each term in $\frac{dE}{dt}$ is negative. Following Ren’s Method, Shen et al. proposed an energy variation method [50, 51] with predefined energetic and dissipative functionals. The unknown terms in the kinematics assumptions are obtained by matching $\frac{dE}{dt}$ with a predefined dissipative function Δ .

In recent years, the variational method has been instrumental in proposing various dynamic boundary conditions that consider the possible short-range interactions of materials with solid walls. For instance, Qian et al. [46, 35] utilized the Onsager principle to establish the general Navier boundary condition (GNBC), which captures the dynamics of contact lines. Furthermore, building upon EnVarA, Liu et al. [37] introduced a new category of dynamic boundary conditions, further generalized in [34]. Most of the existing research has primarily focused on closed systems with no exchanges through the boundary, subsequently incorporating flux conditions as part of the boundary dissipation [46]. However, it’s important to note that a majority of biological systems and all engineered devices are open systems characterized by the flow of flux both into and out of the considered domain. Addressing this, Brunet et al. [10] were the pioneers in considering the mass flux effect using the Onsager variational method in linear electrohydrodynamic responses. Building on this, Xu et al. [68] extended the concept by establishing the generalized Lorentz reciprocal theorem for complex fluids and non-isothermal systems. This paper introduces a thermodynamically consistent framework tailored for open systems. The proposed framework incorporates both energetic and dissipative components at the boundary and within the bulk, while also considering chemical reactions.

The law of mass action [41] is a foundational principle in chemistry that establishes a relationship between the concentrations of reactants and products in an ideal chemical reaction and its equilibrium constant. In recent times, various models have been developed to describe chemical reactions based on the principles of thermodynamics [28, 72, 38]. Wang et al. [63, 62, 36] extended this framework with the EnVarA approach to encompass chemical reaction systems described by rate constants. Our methods extend the pioneering work of Wang et al. [63, 62], who explored reactions not involving charges or electrostatics. This generalization enables us to investigate the influence of electric potential on chemical reaction rates often described by the Butler-Volmer equation [12, 22, 18]. The generalization equips us with the necessary tools for modeling biochemical reactions.

The rest of the paper is organized as follows. In Section 2, we derive the general field theory for open system with flux on the boundary and then the method is use to derive equations for an ionic system with reaction in bulk region, on the boundary and on the interior interface. The simulation

results for a bidomain reaction system are presented in Section 3. The discussions and conclusions are shown in Section 4.

2 Mathematical Models

For a closed system, the First Law of Thermodynamics states that the rate of change of the sum of the kinetic energy \mathcal{K} and the internal energy \mathcal{U} is equal to the sum of the rates of change of work \mathcal{W} and heat \mathcal{Q} , so $\frac{d(\mathcal{K}+\mathcal{U})}{dt} = \frac{d\mathcal{W}}{dt} + \frac{d\mathcal{Q}}{dt}$. In the context of standard statistical physics, the internal energy \mathcal{U} considers the interactions among particles. These interactions can be categorized as either short range, such as hardcore interactions, or long range, such as Coulomb electrostatic interactions. The Second Law of Thermodynamics, in the isothermal case, is given by, $T\frac{d\mathcal{S}}{dt} = \frac{d\mathcal{Q}}{dt} + \Delta$, where T is temperature, \mathcal{S} is entropy and $\Delta \geq 0$ is entropy production. As a reformulation of the linear response assumption, this entropy production functional can be represented as the sum of various rates such as the velocities and the strain rates. By subtracting the Second Law from the First Law, under the isothermal assumption, assuming both laws are valid for nonequilibrium open systems, we have,

$$\frac{dE}{dt} = \frac{d\mathcal{W}}{dt} - \Delta, \quad (1)$$

where $E = \mathcal{K} + \mathcal{F}$ is the total energy and $\mathcal{F} := \mathcal{U} - \mathcal{T}\mathcal{S}$ is the Helmholtz free energy. In case no external forces or fields are applied, i.e. $\frac{d\mathcal{V}}{dt} = 0$, we can derive the dissipation law $\frac{dE}{dt} = -\Delta$.

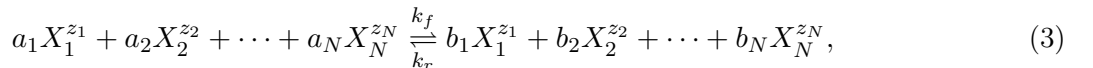
Open systems have some fluxes that flow in or out through the boundary and have distinctive energy dissipation laws that differ from those of closed systems. They have the distinct inputs and outputs that characterize devices in engineering. In open systems, energy can change both because of the flux across the boundary and also because of the change in dissipation. For open systems, we assume the following energy law

$$\frac{dE}{dt} = \mathcal{P}_{E,\partial\Omega} - \Delta, \quad (2)$$

where $\mathcal{P}_{E,\partial\Omega}$ is the energy exchange rate through energy due to the variation of total particles, energy. It is important to note that both the total energy and dissipation functionals incorporate contributions from both the bulk region and the boundary.

2.1 Bulk reaction

We consider a domain that has reactions in bulk and connects to an infinite large reservoir with fixed chemical potential on the boundary. We focus on elementary reactions containing N species $\{X_1^{z_1}, X_2^{z_2}, \dots, X_N^{z_N}\}$



where k_f and k_r are the forward and backward reaction rates, C_i is the concentration of X_i , respectively. Here a_i and b_i are the stoichiometric coefficients, and z_i is the valence of i^{th} species. If let $\gamma_i = b_i - a_i$. Charge conservation implies $\sum_{i=1}^N \gamma_i z_i = 0$.

Based on the law of conservation of mass [17] and Maxwell equations, we have the following kinematic assumptions

$$\begin{cases} \frac{\partial C_i}{\partial t} = -\nabla \cdot \mathbf{j}_i + \gamma_i \mathcal{R}, \\ \nabla \cdot (\mathbf{D}) = \sum_{i=1}^N z_i C_i F, \\ \nabla \times \mathbf{E} = \mathbf{0}, \end{cases} \quad (4)$$

where $\mathbf{j}_i, i = 1, \dots, N$ are the passive fluxes, z_i is the valence of i^{th} particle, F is Faraday constant and $\mathcal{R} = \mathcal{R}_f - \mathcal{R}_r$ is the net reaction rate function with forward and reverse reactions rate \mathcal{R}_f and \mathcal{R}_r . \mathbf{D} is Maxwell's electrical displacement field and $\mathbf{D} = \varepsilon_0 \varepsilon_r \mathbf{E}$ with electric field \mathbf{E} , dielectric constant

ε_0 and relative dielectric constant ε_r . The equation $\nabla \times \mathbf{E} = \mathbf{0}$ implies that there exists an electric potential ϕ such that $\mathbf{E} = -\nabla\phi$.

The boundary conditions are

$$\begin{cases} \mathbf{j}_i \cdot \mathbf{n} = j_{i,ex}, & i = 1 \cdots, N, \quad \text{on } \partial\Omega, \\ \mathbf{D} \cdot \mathbf{n} = 0, & \text{on } \partial\Omega. \end{cases} \quad (5)$$

where $j_{i,ex}$ is the flux of i_{th} ion supplied from an external source and to be determined later with fixed reservoir chemical potential, \mathbf{n} is the unit outward normal vector.

Remark 2.1. By multiplying $z_i F$ on both sides of the first equation, we have

$$\frac{\partial}{\partial t}(\nabla \cdot \mathbf{D}) = \sum_{i=1}^N z_i F \frac{\partial C_i}{\partial t} = - \sum_{i=1}^N \nabla \cdot (z_i F \mathbf{j}_i) + \sum_{i=1}^N z_i F \gamma_i \mathcal{R} = - \sum_{i=1}^N \nabla \cdot (z_i F \mathbf{j}_i) \quad (6)$$

which is consistent with the electrostatic Maxwell equations. Treatment of transient problems, involving displacement currents is needed to deal with some important experimental work [4, 7, 59, 8, 13, 58].

The total energetic functional is defined as the summation of entropies of mixing, internal energy and electrical static energy [55, 63],

$$\begin{aligned} E &= E_{ent} + E_{int} + E_{ele} \\ &= \sum_{i=1}^N \int_{\Omega} RT \left\{ C_i \left(\ln \left(\frac{C_i}{c_0} \right) - 1 \right) \right\} dx + \int_{\Omega} \sum_{i=1}^N C_i U_i dx + \int_{\Omega} \frac{\mathbf{D} \cdot \mathbf{E}}{2} dx, \end{aligned} \quad (7)$$

where R is universal gas constant, T is temperature, U_i is the standard free energy density of i_{th} particle (temperature of 298 K; concentration 1M) [41].

Then the electrochemical potentials (used in the following derivations) are defined by

$$\tilde{\mu}_i = \mu_i + z_i \phi F = RT \ln \frac{C_i}{c_0} + U_i + z_i \phi F, \quad i = 1, \cdots, N. \quad (8)$$

It is assumed in the present work that the dissipation of the system energy is due to passive diffusion and chemical reaction. Additional dissipations (and energies for that matter) can be included if needed in later applications.

$$\Delta = \int_{\Omega} \left\{ \sum_{j=1}^N \frac{RT}{D_j C_j} |\mathbf{j}_j|^2 + RT \mathcal{R} \ln \left(\frac{\mathcal{R}_f}{\mathcal{R}_r} \right) \right\} dx + \sum_{i=1}^N \int_{\partial\Omega} \frac{1}{g_i} |j_{i,ex}|^2 dS, \quad (9)$$

where $\mathcal{R} = \mathcal{R}_f - \mathcal{R}_r$ and g_i is the conductivity of i_{th} species on the boundary.

The boundary energy communication rate $\mathcal{P}_{E,\partial\Omega}$ is induced by the mass communication flux with energy density $\tilde{\mu}_{i,ex}$

$$\mathcal{P}_{E,\partial\Omega} = - \sum_{i=1}^N \int_{\partial\Omega} \tilde{\mu}_{i,ex} j_{i,ex} dS, \quad (10)$$

where $\tilde{\mu}_{i,ex}$ is the fixed chemical potential of i_{th} species $\tilde{\mu}_i$ in the reservoir.

Taking the time derivative of the energy functional (7) yields

$$\begin{aligned} \frac{dE}{dt} &= \int_{\Omega} \sum_{i=1}^N \{ \nabla \tilde{\mu}_i \cdot \mathbf{j}_i \} dx + \int_{\Omega} \mathcal{R} \sum_{i=1}^N \gamma_i \tilde{\mu}_i dx - \int_{\partial\Omega} \sum_{i=1}^N (\tilde{\mu}_i - \tilde{\mu}_{i,ex}) \mathbf{j}_i \cdot \mathbf{n} dS - \int_{\partial\Omega} \tilde{\mu}_{i,ex} \mathbf{j}_i \cdot \mathbf{n} dS. \\ &= -\Delta + \mathcal{P}_{E,\partial\Omega}. \end{aligned} \quad (11)$$

where the detailed derivation can be found in the Appendix.

By comparing with the dissipation function, we have

$$\begin{cases} \mathbf{j}_i = -\frac{D_i}{RT}C_i\nabla\tilde{\mu}_i, & i = 1, \dots, N & \text{in } \Omega \\ \mathbf{j}_i \cdot \mathbf{n} = g_i(\tilde{\mu}_i - \tilde{\mu}_{i,ex}) & & \text{on } \partial\Omega \\ RT \ln\left(\frac{\mathcal{R}_f}{\mathcal{R}_r}\right) = -\sum_{i=1}^N \gamma_i \tilde{\mu}_i = RT \ln\left(\frac{\prod_{i=1}^N \left(\frac{C_i}{c_0}\right)^{a_i}}{\prod_{i=1}^N \left(\frac{C_i}{c_0}\right)^{b_i}} e^{\frac{\Delta U}{RT}}\right), & & \text{on } \partial\Omega. \end{cases} \quad (12)$$

where $A = -\sum_{i=1}^N \gamma_i \tilde{\mu}_i = \sum_{i=1}^N (a_i - b_i) \tilde{\mu}_i$ is the local affinity [16] and the last equation is part of the De Donder-Weyl theory [2, 49].

If we assume the reaction rate function is

$$\mathcal{R} = \mathcal{R}_f - \mathcal{R}_r = k_{f,0} \prod_{i=1}^N \left(\frac{C_i}{c_0}\right)^{a_i} - k_{r,0} \prod_{i=1}^N \left(\frac{C_i}{c_0}\right)^{b_i}$$

where $k_{f,0}$ and $k_{r,0}$ are forward and backward reaction rate constants with unit $\frac{M}{s} = \frac{Mol}{Ls}$ [45], then De Donder-Weyl theory yields

$$\frac{k_{r,0}}{k_{f,0}} = k_{eq} = e^{\frac{-\Delta U}{RT}}, \quad (13)$$

where $\Delta U = \sum_{i=1}^N (a_i - b_i) U_i$ and k_{eq} is the equilibrium constant [45].

The governing equations for the bulk reaction are given as

$$\begin{cases} \frac{\partial C_i}{\partial t} = \nabla \cdot (D_i \nabla C_i + D_i \frac{z_i F}{RT} C_i \nabla \phi) + \gamma_i \left(k_{f,0} \prod_{i=1}^N \left(\frac{C_i}{c_0}\right)^{a_i} - k_{r,0} \prod_{i=1}^N \left(\frac{C_i}{c_0}\right)^{b_i} \right), \\ -\nabla \cdot (\varepsilon_0 \varepsilon_r \nabla \phi) = \sum_{i=1}^N z_i F C_i, \end{cases} \quad (14)$$

with boundary conditions

$$\begin{cases} \mathbf{j}_i \cdot \mathbf{n} = g_i(\tilde{\mu}_i - \tilde{\mu}_{i,ex}), & i = 1 \dots N, & \text{on } \partial\Omega, \\ \mathbf{D} \cdot \mathbf{n} = 0, & & \text{on } \partial\Omega. \end{cases} \quad (15)$$

The energy law of this system could be written as follows

$$\begin{aligned} \frac{dE}{dt} &= -\int_{\Omega} \left\{ \sum_{j=1}^N \frac{D_j C_j}{RT} |\nabla \tilde{\mu}_j|^2 + RT \mathcal{R} \ln\left(\frac{\mathcal{R}_f}{\mathcal{R}_r}\right) \right\} dx - \sum_{i=1}^N \int_{\partial\Omega} g_i |\tilde{\mu}_i - \tilde{\mu}_{i,ex}|^2 dS \\ &\quad - \sum_{i=1}^N \int_{\partial\Omega} g_i \tilde{\mu}_{i,ex} (\tilde{\mu}_i - \tilde{\mu}_{i,ex}) dS \\ &= -\Delta + \mathcal{P}_{E,\partial\Omega}. \end{aligned} \quad (16)$$

Here the boundary condition of concentration is Robin type that allows flux across a boundary ‘resistance’.

- If the boundary conductivity is zero $g_i = 0$, then we obtain the nonflux boundary condition $\mathbf{j}_i \cdot \mathbf{n} = 0$ that describes an insulating boundary and a closed system. The corresponding energy law is

$$\frac{dE}{dt} = -\int_{\Omega} \left\{ \sum_{j=1}^N \frac{D_j C_j}{RT} |\nabla \tilde{\mu}_j|^2 + RT \mathcal{R} \ln\left(\frac{\mathcal{R}_f}{\mathcal{R}_r}\right) \right\} dx = -\Delta. \quad (17)$$

with zero boundary energy communication rate $\mathcal{P}_{E,\partial\Omega} = 0$.

- If the conductance is infinitely large, the Dirichlet boundary condition is achieved $\tilde{\mu}_i = \tilde{\mu}_{i,ex}$ on the boundary. This Dirichlet condition is called a ‘voltage clamp’ in biophysics. Note the voltage clamp is an open system requiring the injection of current and energy provided by an external system usually called a voltage clamp amplifier.

- If the conductance is a function of chemical potential, as may be the case in some membrane proteins, including channels and transporters, i.e. $g_i = \frac{j_{i,0}}{\tilde{\mu}_i - \tilde{\mu}_{i,ex}}$, where $j_{i,0}$ is constant, then we obtain the Neumann boundary condition $\mathbf{j}_i \cdot \mathbf{n} = j_{i,0}$. In this case, the corresponding energy law is

$$\frac{dE}{dt} = - \int_{\Omega} \left\{ \sum_{j=1}^N \frac{D_j C_j}{RT} |\nabla \tilde{\mu}_j|^2 + RT \mathcal{R} \ln \left(\frac{\mathcal{R}_f}{\mathcal{R}_r} \right) \right\} dx - \sum_{i=1}^N \int_{\partial\Omega} \tilde{\mu}_i j_{i,0} dS. \quad (18)$$

Our approach is able to handle a wide range of boundary conditions. For example, it can include complex current, voltage, and concentration relations needed to describe some ion channels and transporters.

2.2 Chemical reactions on the boundary

We now extend our treatment to include chemical reactions on the boundary, for example, as might happen on the surface of a metal electrode

$$a_1 X_1^{z_1} + a_2 X_2^{z_2} + \dots + a_N X_N^{z_N} + \Delta z e^{-1} \frac{k_f}{k_r} b_1 X_1^{z_1} + b_2 X_2^{z_2} + \dots + b_N X_N^{z_N}, \quad (19)$$

where electrons are supplied through surface Γ with the electrode potential ϕ_p and $\sum_{i=1}^N \gamma_i z_i + \Delta z = 0$. For example, if X_1, X_2, \dots, X_k are oxidized species and X_{k+1}, \dots, X_N are reduced species, then $a_{k+1} = a_{k+2} = \dots = a_N = 0$ and $b_1 = b_2 = \dots = b_k = 0$, i.e.

$$a_1 X_1^{z_1} + a_2 X_2^{z_2} + \dots + a_k X_k^{z_k} + \Delta z e^{-1} \frac{k_f}{k_r} b_{k+1} X_{k+1}^{z_{k+1}} + b_{k+2} X_{k+2}^{z_{k+2}} + \dots + b_N X_N^{z_N}, \quad (20)$$

During the derivation, we only focus on situations where the oxidized state exists only in solution near the surface of the metal plate [1] as shown in Fig. 1.

The conservation law yields the following kinematic assumptions,

$$\begin{cases} \frac{\partial C_i}{\partial t} = -\nabla \cdot \mathbf{j}_i, & \text{in } \Omega \\ -\nabla \cdot (\varepsilon_0 \varepsilon_r \nabla \phi) = \sum_{i=1}^N z_i F C_i, & \text{in } \Omega \end{cases} \quad (21)$$

with boundary conditions

$$\begin{cases} \mathbf{j}_i \cdot \mathbf{n} = -\gamma_i \mathcal{R}, i = 1 \dots N, & \text{on } \Gamma, \\ F \frac{\partial C_e}{\partial t} = \mathbb{C}_p \frac{\partial(\phi - \phi_p)}{\partial t} = j_{ex} F - \Delta z F \mathcal{R}, & \text{on } \Gamma \\ \mathbf{j}_i \cdot \mathbf{n} = 0, \phi = 0, & \text{on } \partial\Omega/\Gamma, \end{cases} \quad (22)$$

where C_e is the density of electrons on the surface of the plate, ϕ_p is the electric potential on the plate, and \mathbb{C}_p is the capacitance, I_{ex} is the current supplied by an external amplifier and the corresponding inlet electron flux is $j_{ex} = -\frac{I_{ex}}{F}$. Here we use the fact that $FC_e = \mathbb{C}_p(\phi - \phi_p)$.

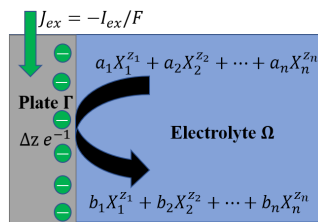


Figure 1: Schematic of reaction on the metal electrode with external electron textcolorblueinput $J_{ex} = -\frac{I_{ex}}{F}$.

Then the total energy is defined as the sum of mix energy and internal energy of ions, electric static energy in the bulk region, and the energy on the interface induced by electrons and capacitor effect

$$\begin{aligned}
E &= E_{ent} + E_{int} + E_{ele} + E_{\Gamma} \\
&= \underbrace{\sum_{i=1}^N \int_{\Omega} \left\{ RT C_i \left(\ln \left(\frac{C_i}{c_0} \right) - 1 \right) + C_i U_i \right\} dx}_{bulk} + \int_{\Omega} \frac{\mathbf{D} \cdot \mathbf{E}}{2} dx \\
&\quad + \underbrace{\int_{\Gamma} \left\{ RT C_e \left(\ln \left(\frac{C_e}{c_{e,0}} \right) - 1 \right) + C_e U_e \right\} dx}_{boundary} + \frac{1}{2} \int_{\Gamma} C_p (\phi - \phi_p)^2 dS. \tag{23}
\end{aligned}$$

where U_i and U_e is the internal energy of i_{th} ion and electron, respectively. Here $c_{e,0}$ is the characteristic density.

Then the corresponding electrochemical potentials of ions and electrons are

$$\tilde{\mu}_i = \mu_i + z_i F \phi = U_i + RT \ln \frac{C_i}{c_0} + z_i F \phi, \tag{24}$$

$$\tilde{\mu}_e = \mu_e - F \phi_p = U_e + RT \ln \frac{C_e}{c_{e,0}} - F \phi_p. \tag{25}$$

The dissipation function is defined as

$$\Delta = \int_{\Omega} \sum_{j=1}^N \frac{D_j C_j}{RT} |\nabla \tilde{\mu}_j|^2 dx + \int_{\Gamma} RT \mathcal{R} \ln \left(\frac{\mathcal{R}_f}{\mathcal{R}_r} \right) dS + \int_{\Gamma} \frac{g}{F^2} (\tilde{\mu}_e - \tilde{\mu}_{ex})^2 dS, \tag{26}$$

where we used the boundary reaction rate function $\mathcal{R} = \mathcal{R}_f - \mathcal{R}_r$, $\tilde{\mu}_{ex}$ is the external electron chemical potential of the reservoir that connects to the boundary.

We analyze a setup (see Fig. 1) with a given current of electrons I_{ex} applied to the plate Γ . This is a flux (really current) boundary condition, of the Neumann type in mathematical language. The other boundaries of the system are controlled in a different way. They are insulators that help isolate the system so it communicates with the outside world in a limited well-defined way. On these insulating boundaries, no ions enter or leave the system on those other boundaries, i.e. $\mathbf{J}_i \cdot \mathbf{n} = 0$, and the electric potential is fixed as ϕ_{ref} . The current flow of electrons is only on the left and the boundary energy power functional is defined as follows

$$\mathcal{P}_{E,\partial\Omega} = \int_{\Gamma} \tilde{\mu}_e j_{ex} dx. \tag{27}$$

Remark 2.2. Integrating the first equation and using the boundary condition on i_{th} ion yields the law of mass conservation

$$\frac{d}{dt} \int_{\Omega} C_i dt = \int_{\Gamma} \gamma_i \mathcal{R} dS. \tag{28}$$

To apply the dissipation theorem, we need the derivative of energy with respect to time.

$$\begin{aligned}
\frac{dE}{dt} &= \int_{\Omega} \sum_{i=1}^N \{ \nabla \tilde{\mu}_i \cdot \mathbf{j}_i \} dx - \int_{\Gamma} \left(- \sum_i \tilde{\mu}_i \gamma_i + \tilde{\mu}_e \Delta z \right) \mathcal{R} dS - \int_{\Gamma} \phi \frac{\partial}{\partial t} (\mathbf{D} \cdot \mathbf{n} - F C_e) dS \\
&\quad + \int_{\Gamma} (\tilde{\mu}_e - \tilde{\mu}_{ex}) j_{ex} dS + \int_{\Gamma} \tilde{\mu}_{ex} J_{ex} dS - \int_{\partial\Omega/\Gamma} \phi \frac{\partial \mathbf{D} \cdot \mathbf{n}}{\partial t} dS - \int_{\partial\Omega/\Gamma} \sum_i \tilde{\mu}_i \mathbf{j}_i \cdot \mathbf{n} dS \\
&= -\Delta + \mathcal{P}_{E,\partial\Omega}, \tag{29}
\end{aligned}$$

where the detailed derivation is presented in the Appendix.

To implement the dissipation principle, we now compare Eq. (29) with the dissipation function defined in Eq. (26). We are dealing with an open system so we include the dissipation (and energy) associated with the boundaries as well as the interior of the system.

$$\begin{cases} \mathbf{j}_i = -\frac{D_i}{RT} C_i \nabla \tilde{\mu}_i, & i = 1, \dots, N, & \text{in } \Omega \\ \mathbf{D} \cdot \mathbf{n} = FC_e & & \text{on } \Gamma \\ j_{ex} = \frac{g}{F^2} (\tilde{\mu}_{ex} - \tilde{\mu}_e), & & \text{on } \Gamma \\ RT \ln \left(\frac{\mathcal{R}_f}{\mathcal{R}_r} \right) = -\sum_i^N \gamma_i \tilde{\mu}_i + \tilde{\mu}_e \Delta z, & & \text{on } \Gamma \\ \mathbf{j}_i \cdot \mathbf{n} = 0, \phi = 0, & & \text{on } \partial\Omega/\Gamma. \end{cases} \quad (30)$$

The third equation in (30) yields

$$\mathcal{R} = \mathcal{R}_f (1 - e^{-\frac{A_e}{RT}}). \quad (31)$$

with the affinity

$$A_e = -\sum_{i=1}^N \gamma_i \tilde{\mu}_i + \Delta z \tilde{\mu}_e = RT \ln \left(\left(\frac{C_e}{c_{e,0}} \right)^{\Delta z} \frac{\prod_{i=1}^N \left(\frac{C_i}{c_0} \right)^{a_i}}{\prod_{i=1}^N \left(\frac{C_i}{c_0} \right)^{b_i} k_{eq}} e^{\frac{\Delta z F}{RT} (\phi - \phi_p)} \right) \quad (32)$$

where $\Delta U = \sum_{i=1}^N (a_i - b_i) U_i + \Delta z U_e$ and $k_{eq} = e^{-\frac{\Delta U}{RT}}$ is used. If we assume

$$\mathcal{R}_f = k_{f,0} \left(\frac{C_e}{c_{e,0}} \right)^{\Delta z} \prod_{i=1}^N \left(\frac{C_i}{c_0} \right)^{a_i} e^{-\frac{\Delta z F}{RT} \beta (\phi_p - \phi)}, \quad (33)$$

then the reaction rate function could be defined as follows

$$\begin{aligned} \mathcal{R} &= \mathcal{R}_f \left(1 - e^{-\frac{\sum_{i=1}^N (a_i - b_i) \tilde{\mu}_i + \Delta z \tilde{\mu}_e}{RT}} \right) \\ &= k_{f,0} e^{-\frac{\Delta z F}{RT} \beta (\phi_p - \phi)} \left(\frac{C_e}{c_{e,0}} \right)^{\Delta z} \prod_{i=1}^N \left(\frac{C_i}{c_0} \right)^{a_i} - k_{r,0} e^{\frac{\Delta z F}{RT} (1-\beta) (\phi_p - \phi)} \prod_{i=1}^N \left(\frac{C_i}{c_0} \right)^{b_i} \\ &= k_{f,0} e^{-\frac{\Delta z F}{RT} \beta (\Delta \phi)} \left(\frac{C_e}{c_{e,0}} \right)^{\Delta z} \prod_{i=1}^N \left(\frac{C_i}{c_0} \right)^{a_i} - k_{r,0} e^{\frac{\Delta z F}{RT} (1-\beta) (\Delta \phi)} \prod_{i=1}^N \left(\frac{C_i}{c_0} \right)^{b_i} \end{aligned} \quad (34)$$

where we denote $\Delta \phi = \phi_p - \phi$ and β is the so called the transfer coefficient commonly found in the Frumkin-Butler-Volmer Equation [6, 49, 56, 57, 25].

It is important to realize that any analysis of boundary behavior requires detail appropriate for the mechanisms of flow across the boundary. In biological cases, these are often not yet known. In the physical case, details are significantly different in each of the many (quite diverse) systems that are described by the Butler-Volmer equation of electrode reactions [6, 49, 56, 57, 25]. The behavior of the systems is likely to be as diverse as the chemical reactions at the boundaries are themselves.

In summary, we have the following system

$$\begin{cases} \frac{\partial C_i}{\partial t} = -\nabla \cdot \mathbf{j}_i, & \text{in } \Omega \\ -\nabla \cdot (\varepsilon_0 \varepsilon_r \nabla \phi) = \sum_{i=1}^N z_i F C_i, & \text{in } \Omega \end{cases} \quad (35)$$

with boundary conditions

$$\begin{cases} \mathbf{j}_i \cdot \mathbf{n} = -\gamma_i \mathcal{R}, & i = 1 \dots N, & \text{on } \Gamma, \\ \mathbb{C}_p \frac{d(\phi - \phi_p)}{dt} = -I_{ex} - \Delta z F \mathcal{R} = \frac{g}{F} (\tilde{\mu}_{ex} - \tilde{\mu}_e) - \Delta z F \mathcal{R}, & & \text{on } \Gamma \\ \mathcal{R} = k_{f,0} e^{-\frac{\Delta z F}{RT} \beta (\Delta \phi)} \left(\frac{C_e}{c_{e,0}} \right)^{\Delta z} \prod_{i=1}^N \left(\frac{C_i}{c_0} \right)^{a_i} - k_{r,0} e^{\frac{\Delta z F}{RT} (1-\beta) (\Delta \phi)} \prod_{i=1}^N \left(\frac{C_i}{c_0} \right)^{b_i}, & & \text{on } \Gamma \\ \mathbf{D} \cdot \mathbf{n} = \mathbb{C}_p (\phi - \phi_p), & & \text{on } \Gamma \\ \mathbf{j}_i \cdot \mathbf{n} = 0, \phi = 0, & & \text{on } \partial\Omega/\Gamma. \end{cases} \quad (36)$$

where the similar boundary conditions are used in [3, 6, 70].

The reaction rate function could be written as

$$\mathcal{R} = k_f \left(\frac{C_e}{c_{e,0}} \right)^{\Delta z} \prod_{i=1}^N \left(\frac{C_i}{c_0} \right)^{a_i} - k_r \prod_{i=1}^N \left(\frac{C_i}{c_0} \right)^{b_i}, \quad (37)$$

where we denote

$$k_f = k_{f,0} e^{-\frac{\Delta z F}{RT} \beta (\Delta \phi)}, \quad (38)$$

$$k_r = k_{r,0} e^{\frac{\Delta z F}{RT} (1-\beta) (\Delta \phi)}, \quad (39)$$

to include the effects of electric potential on the reaction rates.

If we choose $g = \frac{I_0 F}{\bar{\mu}_e - \bar{\mu}_{ex}}$, then the input current is constant I_0 and the condition is changed to be $\mathbb{C}_p \frac{d(\phi - \phi_p)}{dt} = -I_0 - \Delta z F \mathcal{R}$ which is the set of boundary condition found widely in the literature [39, 56, 40, 9]. This is based on Kirchhoff's Laws that the input current is either stored in the capacitor or consumed by the reaction.

Remark 2.3. Since $C_e^s = \frac{\mathbb{C}_p}{F} (\phi^s - \phi_p^s)$ is the charge density, it should be nonnegative during evolution, which means $\phi^s > \phi_p^s \geq 0$ for $\forall t \geq 0$.

Remark 2.4. If there is no chemical reaction on the surface Γ , the model degenerates to PNP with dynamic boundary condition

$$\begin{cases} \frac{\partial C_i}{\partial t} = -\nabla \cdot \mathbf{j}_i, & \text{in } \Omega \\ -\nabla \cdot (\varepsilon_0 \varepsilon_r \nabla \phi) = \sum_{i=1}^N z_i F C_i, & \text{in } \Omega \end{cases} \quad (40)$$

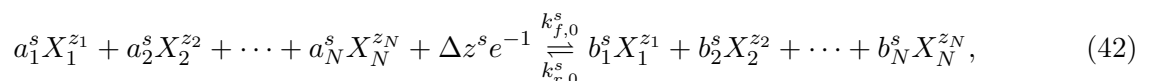
with boundary conditions

$$\begin{cases} \mathbf{j}_i \cdot \mathbf{n} = 0, & i = 1 \cdots N, & \text{on } \partial\Omega, \\ \mathbb{C}_p \frac{d(\phi - \phi_p)}{dt} = -I_{ex}, & & \text{on } \Gamma, \\ \mathbf{D} \cdot \mathbf{n} = \mathbb{C}_p (\phi - \phi_p), & & \text{on } \Gamma, \\ \phi = 0, & & \text{on } \partial\Omega/\Gamma. \end{cases} \quad (41)$$

2.3 A bi-reaction system

We will now apply these general principles to a specific system of significant interest in biological applications, such as the electron transport chain (ETC) on the mitochondrial membrane [30, 76, 65, 64]. The electron transport chain (ETC) is a series of biochemical reactions occurring in the inner mitochondrial membrane of eukaryotic cells or the plasma membrane of prokaryotic cells. It plays a pivotal role in cellular respiration, which is the process by which cells convert nutrients (such as glucose) into energy (in the form of ATP). During the ETC, electrons transfer from electron donors (e.g., NADH and FADH₂) to electron acceptors (e.g., oxygen) through a series of redox reactions. This electron transfer is accompanied by the pumping of protons (H⁺) across the inner mitochondrial or plasma membrane, creating an electrochemical gradient used to generate ATP. Oxidation occurs through a sequence of chemical reactions catalyzed by membrane proteins that connect electron flow on one side of a membrane to a chemical reaction on the other. In essence, the reaction on one side of the plate generates electrons, which are subsequently consumed by the reaction on the other side. This scheme is visually represented in Fig. 2, where the output of the left domain reaction is $|\Delta z_l| e^{-1}$ electrons and the input of the right domain is $|\Delta z_r| e^{-1}$ electrons.

To model this system, we set the domain Ω as a union of two subdomains denoted as Ω_s , where $s = l, r$, separated by the plate Γ . The plate functions analogously to a cell membrane, allowing the conduction of electrons along with a displacement current through the effective membrane capacitance \mathbb{C}_p . The thickness of the plate is negligible when compared to the size of the domain. Within these two compartments Ω_s , where $s = l, r$, there exist a total of N species, represented as $\{X_1^{z_1}, X_2^{z_2}, \dots, X_N^{z_N}\}$, with associated reactions as follows:



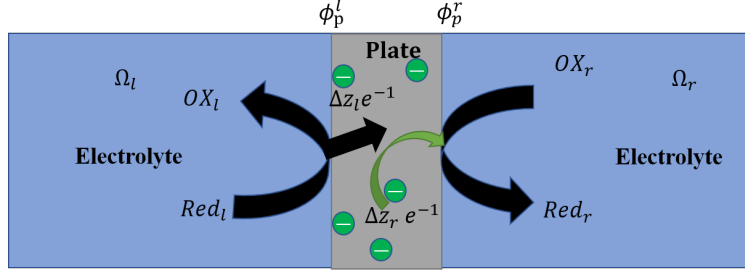


Figure 2: Schematic of Bi-reaction system. On the right side of the plate, the reduction reaction consumes the electrons that are produced by the oxidation reaction on the left side of the plate.

where $k_{f,0}^s$ and $k_{r,0}^s$ are the intrinsic forward and backward reaction rates. In the left region Ω_l , where $\Delta z^l < 0$, this signifies the forward reaction as oxidation, a process that generates electrons. In the right compartment Ω_r , where $\Delta z^r > 0$, this indicates that the forward reaction is a reduction process, consuming electrons.

In the electrolyte region Ω_s , we have the following kinematic assumption

$$\begin{cases} \frac{\partial C_i^s}{\partial t} = -\nabla \cdot \mathbf{j}_i^s, \\ -\nabla \cdot (\varepsilon_0 \varepsilon_r \nabla \phi^s) = \sum_{i=1}^N z_i F C_i^s \end{cases} \quad (43)$$

with the boundary conditions

$$\begin{cases} \mathbf{j}_i^s \cdot \mathbf{n}_s = -\gamma_i \mathcal{R}^s, & \text{on } \Gamma, \\ \mathbb{C}_p \frac{d(\phi^l - \phi_p^l)}{dt} = -\Delta z^l F \mathcal{R}_l + I_{ex}, \mathbb{C}_p \frac{d(\phi^r - \phi_p^r)}{dt} = -\Delta z^r F \mathcal{R}_r - I_{ex}, & \text{on } \Gamma, \\ \mathbf{j}_i^s \cdot \mathbf{n} = 0, & \text{on } \partial\Omega \setminus \Gamma, \end{cases} \quad (44)$$

where the second equation is based on Kirchhoff's Laws and I_{ex} represents the current passing through the plate due to electron transportation.

The total energy is defined as the sum of energy within the two subdomains and on the interface

$$\begin{aligned} E &= E_l + E_r + E_\Gamma \\ &= \sum_{i=1}^N \int_{\Omega^l} \left\{ RT C_i^l \left(\ln \left(\frac{C_i^l}{c_0} \right) - 1 \right) + C_i^l U_i \right\} dx + \int_{\Omega^l} \frac{\mathbf{D}^l \cdot \mathbf{E}^l}{2} dx \\ &\quad + \sum_{i=1}^N \int_{\Omega^r} \left\{ RT C_i^r \left(\ln \left(\frac{C_i^r}{c_0} \right) - 1 \right) + C_i^r U_i \right\} dx + \int_{\Omega^r} \frac{\mathbf{D}^r \cdot \mathbf{E}^r}{2} dx \\ &\quad + \int_\Gamma \left\{ RT C_e^l \left(\ln \left(\frac{C_e^l}{c_{e,0}} \right) - 1 \right) + C_e^l U_e^l \right\} dx + \frac{1}{2} \int_\Gamma \mathbb{C}_p (\phi^l - \phi_p^l)^2 dS \\ &\quad + \int_\Gamma \left\{ RT C_e^r \left(\ln \left(\frac{C_e^r}{c_{e,0}} \right) - 1 \right) + C_e^r U_e^r \right\} dx + \frac{1}{2} \int_\Gamma \mathbb{C}_p (\phi^r - \phi_p^r)^2 dS. \end{aligned} \quad (45)$$

Similarly, the dissipative function is defined as

$$\begin{aligned} \Delta &= \Delta_l + \Delta_r + \Delta_\Gamma \\ &= \int_{\Omega^l} \sum_{j=1}^N \frac{D_j C_j^l}{RT} |\nabla \tilde{\mu}_j^l|^2 dx + \int_\Gamma RT \mathcal{R}^l \ln \left(\frac{\mathcal{R}_f^l}{\mathcal{R}_r^l} \right) dx \\ &\quad + \int_{\Omega^r} \sum_{j=1}^N \frac{D_j C_j^r}{RT} |\nabla \tilde{\mu}_j^r|^2 dx + \int_\Gamma RT \mathcal{R}^r \ln \left(\frac{\mathcal{R}_f^r}{\mathcal{R}_r^r} \right) dx + \int_\Gamma \frac{g(C_e^l)}{F^2} (\tilde{\mu}_e^l - \tilde{\mu}_e^r)^2 dS. \end{aligned} \quad (46)$$

For the boundary input energy power, it is assumed to be

$$\mathcal{P}_{E,\partial\Omega} = - \int_{\partial\Omega} \phi_{ref} \frac{\partial \mathbf{D} \cdot \mathbf{n}}{\partial t} dx. \quad (47)$$

Taking the time derivative of the total energy yields

$$\begin{aligned}
\frac{dE}{dt} - \mathcal{P}_{E,\partial\Omega} &= \int_{\Omega_l} \sum_{i=1}^N \nabla \tilde{\mu}_i^l \cdot \mathbf{j}_i^l dx - \int_{\Gamma} \left(- \sum_{i=1}^N \tilde{\mu}_i^l \gamma_i \mathcal{R}^l + \tilde{\mu}_e^l \Delta z^l \right) \mathcal{R}_l dS - \int_{\Gamma} \phi_l \frac{\partial}{\partial t} (\mathbf{D}^l \cdot \mathbf{n}^l - FC_e^l) dS \\
&+ \int_{\Omega_r} \sum_{i=1}^N \nabla \tilde{\mu}_i^r \cdot \mathbf{j}_i^r dx - \int_{\Gamma} \left(- \sum_{i=1}^N \tilde{\mu}_i^r \gamma_i + \Delta z^r \tilde{\mu}_e^r \right) \mathcal{R}^r dS \\
&- \int_{\Gamma} \phi_r \frac{\partial}{\partial t} (\mathbf{D}^r \cdot \mathbf{n}^r - FC_e^r) dS + \int_{\Gamma} (\tilde{\mu}_e^r - \tilde{\mu}_e^l) J_e - \int_{\partial\Omega} (\phi - \phi_{ref}) \frac{\partial \mathbf{D} \cdot \mathbf{n}}{\partial t} dS \\
&= -\Delta.
\end{aligned} \tag{48}$$

Matching terms yield

$$\left\{ \begin{array}{ll} \mathbf{j}_i^s = -\frac{D_i^s C_i^s}{RT} \nabla \tilde{\mu}_i^s, & \text{in } \Omega^s \\ \mathcal{R}^l = k_{f,0}^l e^{-\frac{\Delta Z F}{RT} \beta (\Delta \phi^l)} \prod_{i=1}^N \left(\frac{C_i^l}{c_0} \right)^{a_i} - k_{r,0}^l e^{\frac{\Delta z^l F}{RT} (1-\beta) (\Delta \phi^l)} \prod_{i=1}^N \left(\frac{C_i^l}{c_{e,0}} \right)^{-\Delta z^l} \left(\frac{C_i^l}{c_0} \right)^{b_i} & \text{on } \Gamma^l \\ \mathcal{R}^r = k_{f,0}^r e^{-\frac{\Delta Z F}{RT} \beta (\Delta \phi^r)} \left(\frac{C_e^r}{c_{e,0}} \right)^{\Delta z^r} \prod_{i=1}^N \left(\frac{C_i^r}{c_0} \right)^{a_i} - k_{r,0}^r e^{\frac{\Delta z^r F}{RT} (1-\beta) (\Delta \phi^r)} \prod_{i=1}^N \left(\frac{C_i^r}{c_0} \right)^{b_i} & \text{on } \Gamma^r \\ \mathbf{D}^s \cdot \mathbf{n}^s = C_e^s F = \mathbb{C}_p (\phi^s - \phi_p^s), & \text{on } \Gamma \\ J_e = -\frac{g}{F^2} (\tilde{\mu}_e^r - \tilde{\mu}_e^l), & \text{on } \Gamma \\ \phi = \phi_{ref}, & \text{on } \partial\Omega/\Gamma. \end{array} \right.$$

In summary, the bidomain reaction system is

$$\left\{ \begin{array}{ll} \frac{\partial C_i^s}{\partial t} = \nabla \cdot \left(\frac{D_i^s C_i^s}{RT} \nabla \tilde{\mu}_i^s \right), & \text{in } \Omega^s \\ -\nabla \cdot (\varepsilon_0 \varepsilon_r \nabla \phi^s) = \sum_{i=1}^N z_i F C_i^s, & \text{in } \Omega^s \end{array} \right. \tag{49}$$

for the boundary conditions

$$\left\{ \begin{array}{ll} \mathbf{j}_i^s \cdot \mathbf{n}_s = -\gamma_i \mathcal{R}^s, & \text{on } \Gamma, \\ \mathcal{R}^l = k_{f,0}^l e^{-\frac{\Delta Z F}{RT} \beta (\Delta \phi^l)} \prod_{i=1}^N \left(\frac{C_i^l}{c_0} \right)^{a_i} - k_{r,0}^l e^{\frac{\Delta z^l F}{RT} (1-\beta) (\Delta \phi^l)} \prod_{i=1}^N \left(\frac{C_i^l}{c_{e,0}} \right)^{-\Delta z^l} \left(\frac{C_i^l}{c_0} \right)^{b_i} & \text{on } \Gamma^l \\ \mathcal{R}^r = k_{f,0}^r e^{-\frac{\Delta Z F}{RT} \beta (\Delta \phi^r)} \left(\frac{C_e^r}{c_{e,0}} \right)^{\Delta z^r} \prod_{i=1}^N \left(\frac{C_i^r}{c_0} \right)^{a_i} - k_{r,0}^r e^{\frac{\Delta z^r F}{RT} (1-\beta) (\Delta \phi^r)} \prod_{i=1}^N \left(\frac{C_i^r}{c_0} \right)^{b_i} & \text{on } \Gamma^r \\ \mathbb{C}_p \frac{d(\phi^l - \phi_p^l)}{dt} = -\Delta z^l F \mathcal{R}^l + \frac{g}{F} (\tilde{\mu}_e^r - \tilde{\mu}_e^l), \mathbb{C}_p \frac{d(\phi^r - \phi_p^r)}{dt} = -\Delta z^r F \mathcal{R}^r - \frac{g}{F} (\tilde{\mu}_e^r - \tilde{\mu}_e^l), & \text{on } \Gamma, \\ \mathbf{D}^s \cdot \mathbf{n}^s = \mathbb{C}_p (\phi^s - \phi_p^s), & \text{on } \Gamma, \\ \mathbf{j}_i^s \cdot \mathbf{n} = 0, \phi = \phi_{ref} & \text{on } \partial\Omega \setminus \Gamma. \end{array} \right. \tag{50}$$

One of the crucial properties of cell membranes is their voltage-gated mechanisms [14]. These mechanisms encompass a category of membrane proteins, known as ion channels, which are highly responsive to variations in the electric potential difference across a cell's membrane. These ion channels play a pivotal role in various physiological processes within neurons, muscles, and other excitable cells. Their significance lies in their ability to initiate and propagate electrical signals, including action potentials, which are fundamental for nerve cell communication [5] and muscle contraction [42]. Various models, such as the Hodgkin-Huxley model [32], have been proposed to describe voltage-gated mechanisms.

For the sake of simplicity, we model these mechanisms by introducing a potential difference threshold, denoted as θ_0 , using a hard switch

$$g = \begin{cases} g_0 & \text{if } \phi_p^r - \phi_p^l > \theta_0; \\ 0 & \text{otherwise,} \end{cases} \tag{51}$$

or a soft one

$$g = g_0 \tanh \left(\frac{(\phi_p^r - \phi_p^l) - \theta_0}{\epsilon} \right), \tag{52}$$

where g_0 is the maximum conductance and ϵ is the relaxation. Then, when the difference of potential between the two sides of the plate is large enough, the plate becomes conductive and the electron is transported.

3 Results

In the simulation, we consider the 1D computation domain and the plate is in the middle. On the left side of the plate, we have

$$X_1^+ + X_2^{2-} \xrightleftharpoons[k_r^l]{k_f^l} X_3 + e^-.$$

On the right side of the plate,

$$X_4^{2+} + X_5^- + e^- \xrightleftharpoons[k_r^r]{k_f^r} X_6.$$

Let's introduce the following characteristic values: $L = 4.3 \times 10^{-1} \mu\text{m}$, $c_0 = 1 \text{ mM}$, $c_{e,0} = \frac{C_p RT}{F^2} = 4.35 \times 10^2 \text{ mol}/\mu\text{m}^2$, $D^* = 10^{-9} \text{ m}^2/\text{s}$, $t^* = \frac{L^2}{D^*} = 1.85 \times 10^{-4} \text{ s}$, $\frac{RT}{F} = 25.6 \text{ mv}$, and $k_f^* = 2.33 \times 10^4 \text{ M/s}$. These values represent the characteristic length, concentration, electron density, diffusion constant, time, electric potential, and reaction rate, respectively. With these characteristic values, we can derive the dimensionless system as follows.

$$\begin{cases} \frac{\partial C_i^s}{\partial t} = \nabla \cdot (D_i^s (\nabla C_i^s + z_i C_i^s \nabla \phi^s)), \\ -\nabla \cdot (\delta^2 \nabla \phi^s) = \sum_{i=1}^N z_i C_i^s, \end{cases} \quad (53)$$

with the boundary conditions

$$\begin{cases} \mathbf{j}_i^s \cdot \mathbf{n}_s = -\gamma_i \zeta \mathcal{R}^s, & \text{on } \Gamma, \\ -\nabla \phi_s \cdot \mathbf{n}_s = \lambda_s (\phi^s - \phi_p^s), & \text{on } \Gamma, \\ \frac{\partial}{\partial t} (-\nabla \phi_l \cdot \mathbf{n}_l) + \frac{\zeta}{\delta^2} \Delta z_l \mathcal{R}_l = g \left(\ln \left(\frac{C_e^r}{C_e^l} \right) + \phi_p^l - \phi_p^r \right), & \text{on } \Gamma, \\ \frac{\partial}{\partial t} (-\nabla \phi_r \cdot \mathbf{n}_r) + \frac{\zeta}{\delta^2} \Delta z_r \mathcal{R}_r = -g \left(\ln \left(\frac{C_e^r}{C_e^l} \right) + \phi_p^l - \phi_p^r \right), & \text{on } \Gamma, \\ \mathbf{j}^s \cdot \mathbf{n} = 0, \phi^s = 0, & \text{on } \partial\Omega/\Gamma, \end{cases} \quad (54)$$

where

$$\begin{aligned} \mathcal{R}^l &= k_{f,0}^l e^{-\Delta Z_l \beta (\phi_p^l - \phi^l)} \prod_{i=1}^N (C_i^l)^{a_i} - k_{r,0}^l e^{\Delta Z_l (1-\beta) (\phi_p^l - \phi^l)} (C_e^l)^{-\Delta z^l} \prod_{i=1}^N (C_i^l)^{b_i} \\ &= k_f^l \prod_{i=1}^N (C_i^l)^{a_i} - k_r^l (C_e^l)^{-\Delta z^l} \prod_{i=1}^N (C_i^l)^{b_i} \\ \mathcal{R}^r &= k_{f,0}^r e^{-\Delta Z_r \beta (\phi_p^r - \phi^r)} (C_e^r)^{\Delta z^r} \prod_{i=1}^N (C_i^r)^{a_i} - k_{r,0}^r e^{\Delta Z_r (1-\beta) (\phi_p^r - \phi^r)} \prod_{i=1}^N (C_i^r)^{b_i} \\ &= k_f^r (C_e^r)^{\Delta z^r} \prod_{i=1}^N (C_i^r)^{a_i} - k_r^r \prod_{i=1}^N (C_i^r)^{b_i} \end{aligned}$$

with $k_f^s = k_{f,0}^s e^{-\Delta Z_s \beta (\phi_p^s - \phi^s)}$ and $k_r^s = k_{r,0}^s e^{\Delta Z_s (1-\beta) (\phi_p^s - \phi^s)}$.

Here $\delta = \frac{\lambda_D}{L}$ is the ratio between Debye length $\lambda_D = \sqrt{\frac{RT \epsilon_0 \epsilon_r}{F^2 c_0}}$ and macroscale length; $\zeta = \frac{k_f^* L}{D^* c_0}$ is the ratio between the reaction time and diffusion time; $\lambda_s = \frac{C_s L}{\epsilon_0 \epsilon_r}$ is the ratio between macroscale length and effective width for the Stern layer; and $g = \frac{g t^* L}{\epsilon_0 \epsilon_r}$ is the ratio between the diffusion time and electric conduction time.

The initial concentrations and dimensionless parameters are set to be $C_1(t=0) = 1$, $C_2(t=0) = \frac{1}{2}$, $C_3(t=0) = 0$, $C_4(t=0) = \frac{1}{2}$, $C_5(t=0) = 1$, $C_6(t=0) = 0$, $\delta = 0.1$, $g = 0.1$, $k_{r,0}^l = k_{r,0}^r = 0.001$. The results in the remaining part of the paper are presented in a dimensionless format.

3.1 Equal intrinsic reaction rates

We first consider the simplified case that the left and right reactions with the same intrinsic reaction rate, $k_{f,0}^l = k_{f,0}^r = 1$. Fig. 3 shows the results of the dynamics of reaction rates, electron density, concentrations of substances, and conductance over time with different time-scale ratio $\zeta = 0.1$ (diffusion dominates), $\zeta = 1$ (diffusion-reaction equal), $\zeta = 10$ (reaction dominates).

As shown in Fig. 3a, the left reaction can be seen as a source—an input—that continually produces electrons until one of the reactants, in this case, X_2 , is depleted. X_2 is the output. (3c). The electrons generated on the left are transported to the right side by the electrochemical potential difference, subsequently driving the reaction on the right side, the output side. Eventually, the output reaction achieves equilibrium after the switch turns off. (Fig. 3b).

As time-scale ratio ζ increases, the reaction rate also increases (Fig. 3a). The reactants on the left plates are consumed much faster (Fig. 3c left) and more electrons accumulate on the left side of the plates (Fig. 3b). The electric potential difference between two sides of the plates $\phi_p^r - \phi_p^l$ increases and opens the gate so that electrons are transported to the right side of the plate (Fig. 3b,d). Then the right reaction starts (3c right). Due to the transport of electrons, the difference in potential between two sides of the plate decreases. The switch then turns off producing the gating dynamics shown in Fig. 3d. Since the total amounts of reactants on the left region are limited, the left reaction stops after a period of time because it runs out of electrons. Without a supply of electrons, the switch turns and the right-side reaction stops. The larger ζ is, the earlier the reaction stops and the switch turns off. The molecular mechanism of the switch remains to be investigated. It resembles the gate of ion channels and may have the same molecular basis [26].

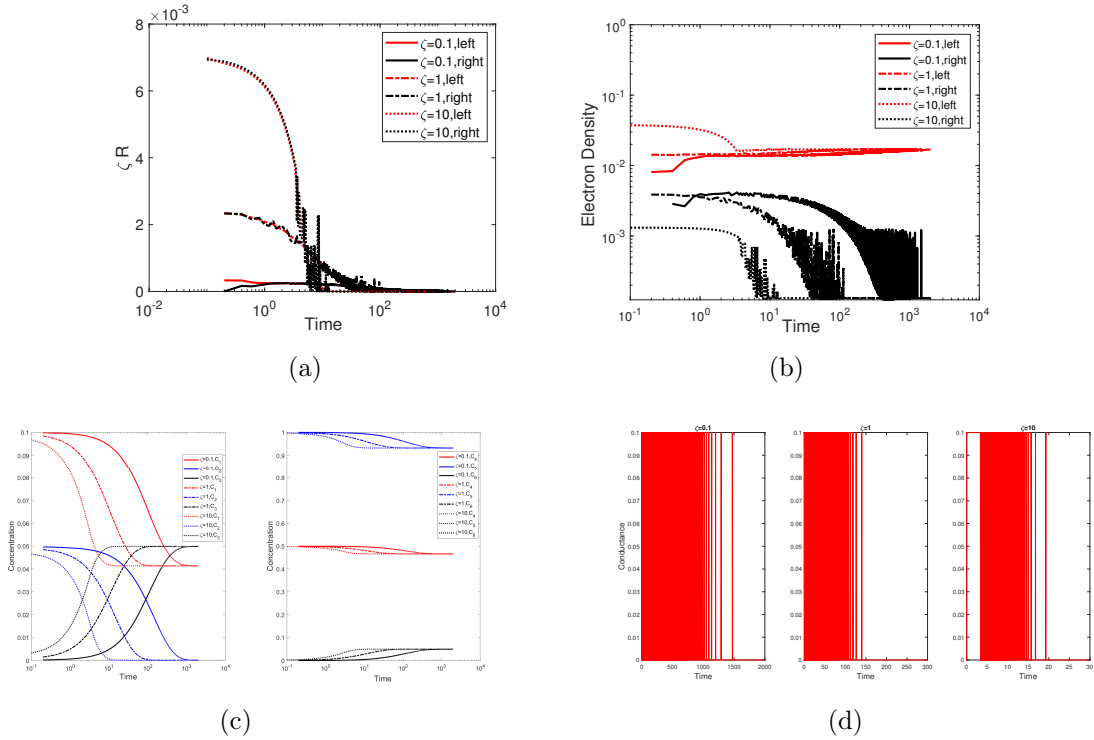


Figure 3: Dynamics evolution of (a) Reaction rates (b) Electron Density (c) Substance concentrations and (d) Conductance changes over time with the same intrinsic reaction rate $k_{f,0}$ on both sides of the plate and different timescale ratio ζ . The results show that the reaction on the left side of the plate is responsible for generating electrons, which are subsequently consumed by the reaction on the right side. The larger ζ is, the earlier the switch turns off and the reaction achieves equilibrium. Dimensional units are used as defined in the beginning of the Results Section.

In Fig. 4, we show how the reaction rate k_f^s changes with electric potential difference $\Delta\phi^s = \phi_p^s - \phi_s$,

i.e. the phase portraits, in Eq.(38). The squares and triangles are the start points and end points of the phase portraits, respectively. $k_{f,0}^s$ is the intrinsic rate constant shown as the solid black line in the figure. When the electric potentials vary with time, the forward reaction rates on the plate vary correspondingly. Since $\Delta z_l < 0$ and $\phi_p^l < \phi_s^l$, then the reaction rate on the left plate is smaller than the reference value $k_{f,0}^l$. On the right plate, since $\Delta z_r > 0$, the reaction rate is always greater than the reference value $k_{f,0}^r$. In summary, the electric potential inhibits the oxidation reaction on the left-hand input side, while accelerating the reduction reaction on the output right-hand side.

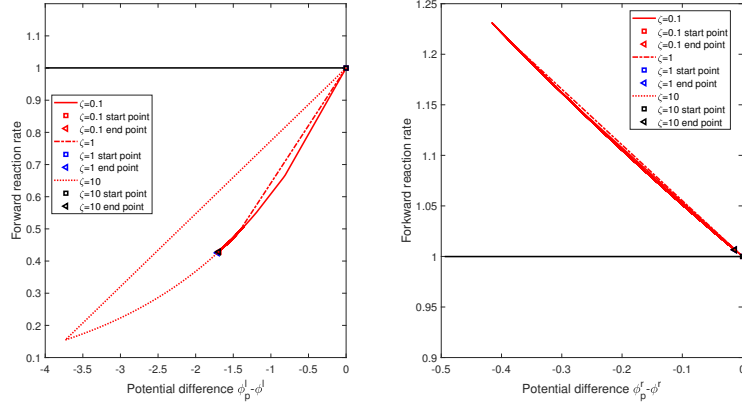


Figure 4: Phase portraits of Reaction rate k_f^s and electric potential difference $\phi_p^l - \phi_l$. Left: left plate; Right: right plate. The black line is the intrinsic forward reaction rate value $k_{f,0}^s = 1, s = l, r$. The squares are the start points and the triangles are the endpoints of the phase portraits. It shows that the electric potential inhibits the oxidation reaction while accelerating the reduction reaction. Dimensional units are used as defined in the beginning of the Results Section.

The spatial distributions of electric potential and concentrations in two regions at equilibrium are shown in Fig. 5. For different ζ , the equilibrium is almost the same. The electric potentials on two sides of the plate ϕ_p^s are lower than the potentials of the electrolyte ϕ^s due to the existence of capacitors. The left plate potential is lower than the potential on the right plate due to the accumulation of electrons. Since C_3 and C_6 are neutral particles, they are uniformly distributed in sapce. The distributions of cations and anions are changed by the electric field.

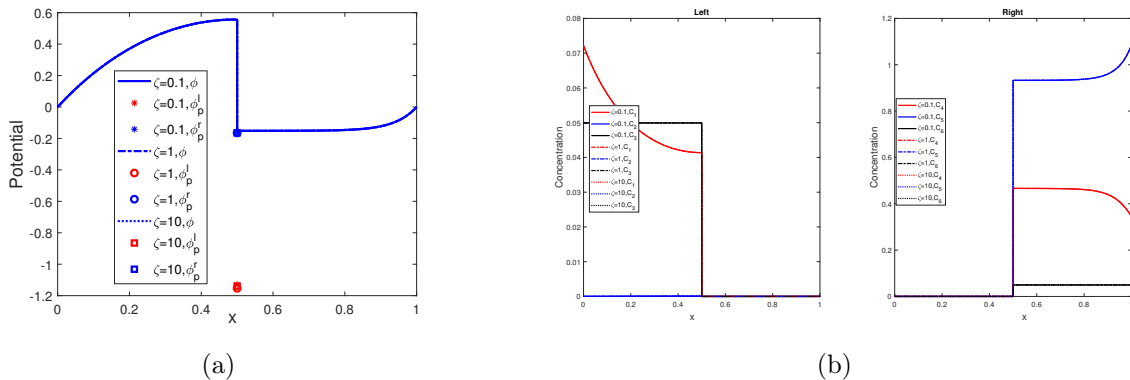


Figure 5: Space distributions of (a) Electric potential; (b) Substance concentrations at equilibrium with the same intrinsic reaction rate $k_{f,0}$ on both sides of the plate and different timescale ratio ζ . Dimensional units are used as defined in the beginning of the Results Section.

In Fig. 6 and Fig. 7, we compare the results with different effective capacitance λ_s . The reaction rate increases as the capacitance increases. And more electrons could be stored on the capacitors.

At the equilibrium, due to larger capacitance, the electric potential difference between the two sides electrolyte decreases. The effect on the spatial distributions of substances at equilibrium is mainly on the left region due to the decrease of electric potential difference.

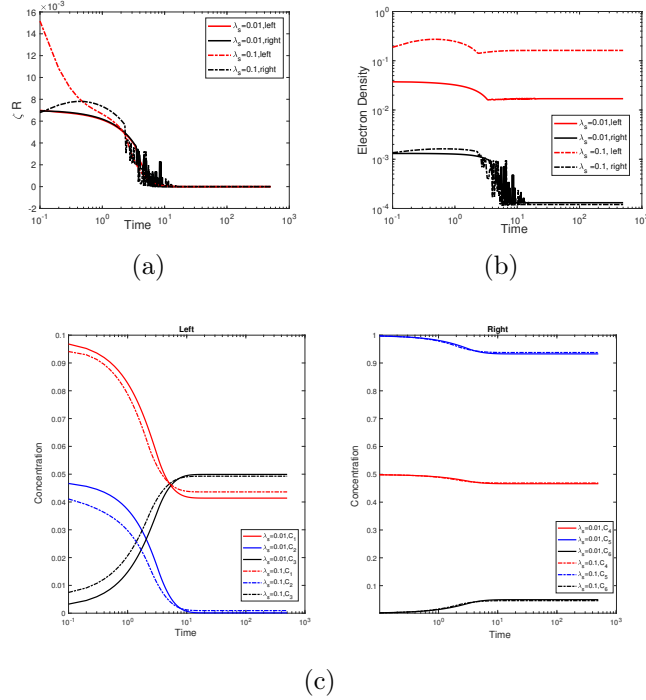


Figure 6: Dynamics evolution of (a) Reaction rates (b) Electron Density (c) Substance concentrations over time with the same intrinsic reaction rate $k_{f,0}$ on both sides of the plate and different capacitance λ_s . Here $\zeta = 10$ is fixed. Dimensional units are used as defined in the beginning of the Results Section.

Because the mechanism of the switch is not known, we investigate two types, a soft switch and a hard switch. In Fig. 8, we present the results obtained when utilizing the soft switch function (52) with $\epsilon = 0.001$. As shown in Fig. 8a-b, a comparison with the hard switch reveals that the right reaction rate function \mathcal{R}_r exhibits a smoother behavior, particularly noticeable for reaction-dominated case ($\zeta = 10$). This smoothing effect arises from the gradual transition around the threshold, allowing the switch to remain in an open state for an extended duration. Consequently, electrons can be transported continuously from the left to the right.

3.2 Different intrinsic reaction rates

In this subsection, we explore the more general scenario where the intrinsic reaction rates on the left and right sides differ, i.e., $k_{f,0}^l \neq k_{f,0}^r$. We maintain a fixed effective capacitance $\lambda_s = 0.1$ and a diffusion-reaction time scale ratio $\zeta = 1$. The outcomes are presented in Fig. 9, where solid lines represent the left-fast-right-slow case ($k_{f,0}^l = 1, k_{f,0}^r = 0.1$), dash-dot lines correspond to the left-slow-right-fast case ($k_{f,0}^l = 0.1, k_{f,0}^r = 1$), and dot lines represent the equal reaction case ($k_{f,0}^l = 1, k_{f,0}^r = 1$).

When the left forward reaction rate constant is faster than the right one, electrons accumulate on the left plate more rapidly at the beginning. Consequently, the left plate reaction initially lags behind compared to the equal reaction case ($k_{f,0}^l = k_{f,0}^r = 1$). The accumulated electrons activate the gate earlier than the slower accumulation (Fig. 9d). In cases where substances are rapidly depleted in the left region (Fig. 9c), the switch is closed. Since the right side forward reaction is slow ($k_{f,0}^r = 0.1$), electrons accumulate on the right plates (Fig. 9d) and maintain the right reaction smoothly even after the gate is closed (Fig. 9a).

In contrast, when the left forward reaction rate constant is slower than the right one, the electron density on the left plate increases more gradually. When the gate is open, the electrons are transported

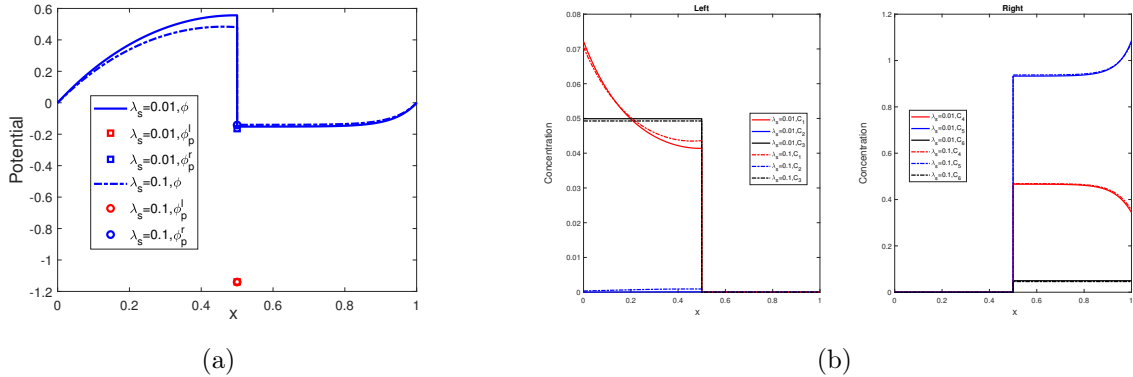


Figure 7: Space distributions of (a) Electric potential; (b) Substance concentrations at equilibrium with the same intrinsic reaction rate $k_{f,0}$ on both sides of the plate and different capacitance λ_s . Here $\zeta = 10$ is fixed. Dimensional units are used as defined in the beginning of the Results Section.

to the right *side*, initiating the reaction on the right later than in the other two cases (Fig. 9a). Simultaneously, since the right forward reaction rate is high, electrons are consumed rapidly, inducing high oscillations in the reaction function on the right plate and leading to high-frequency gating.

4 Discussion and Conclusion

This paper seeks to combine the classical description of electrochemical reactions with a general variational method. Based on the first and second laws of thermodynamics, we generalized the energy variation method [50, 51] for an open system with mass flux communication on the boundary. Then the framework is used to study the chemical reaction in electrolytes where the charges are taken into consideration. When the reaction is only in the bulk region, and not at the membrane, the model obtained is a Poisson-Nernst-Planck (PNP) system with reaction terms that could be taken as a generalized version of the diffusion-reaction model in [63].

Then we consider the reactions on the boundary with current supplied from an external source. Note that our bidomain model (with different reactions on each side of the membrane) forms a self-regulatory reaction system. The effect of electric potential on the reaction rate is consistently modeled with a version of the Frumkin-Butler-Volmer Equation [6, 49, 56, 57, 25].

Next, we analyze a bidomain model with (1) oxidation on the left input side that produces electrons and (2) reduction on the right output side that consumes electrons. Transport across the membrane of conduction and displacement current is included.

We analyze this system because it plays an important role in ATP production and the transport of oxygen/carbon dioxide in living systems. Serious disruption in these reactions is likely to be lethal. Small disruptions lead to a range of health problems, including anemia, sickle cell disease, and other blood disorders.

The simulation results are used to illustrate the diffusion-reaction competition and how the electric potential affects the reaction rate function. In order to model the gating phenomena, we presented simple both hard switch and soft switch models that assume the conductivity of the interface depends on the electric potential difference like the Hodgkin-Huxley model [33, 31].

Our treatment, however, uses only the simplest representations of the chemical reactions themselves and we are quite aware that the specifics of the reactions that have been so exhaustively analyzed in the electrochemistry literature will need to be introduced to our current based models as more realism is sought. Different systems in electrochemistry have different mechanisms. Different systems in biology are also likely to use somewhat different mechanisms for the reactions and the switch, with different regulation.

In this regard, it will be of particular interest to biologists to consult the literature on proton-

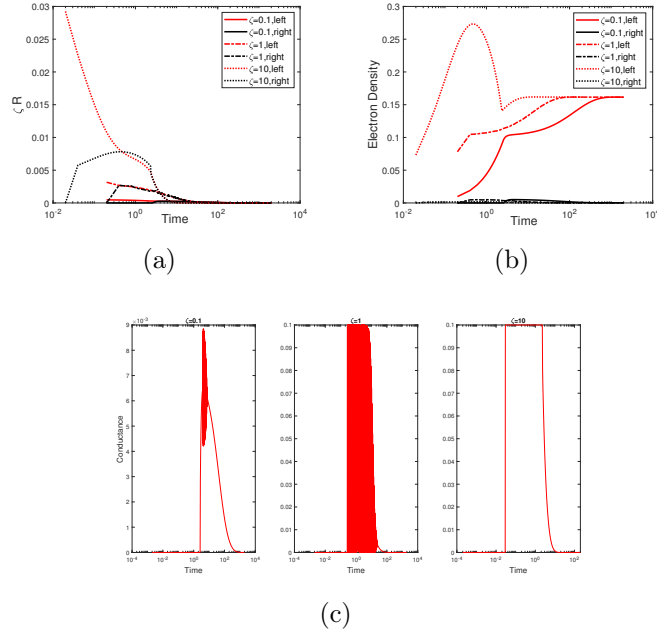


Figure 8: Results with soft switch function. Dynamics evolution of (a) Reaction rate; (b) Electron density; (c) Conductance with fixed $\lambda_s = 0.1$ and different timescale ratio ζ . Dimensional units are used as defined in the beginning of the Results Section.

electron reactions in inorganic systems [25]. In the future, with more detailed information on the reactions and biological structure, our model could be used to study the full electron transport chain during the ATP production that occurs in almost every cell in an animal and other processes, perhaps including the blood clotting cascade process [69, 53].

Chemical reactions can also play an important role in the active motion of soft matter. For example, in some active gels, chemical reactions between the gel components can generate mechanical stress that drives the motion of the gel. Similarly, chemical reactions can be used to generate motion in droplets or other active soft matter systems. Also, in the current work, the fluid is neglected temporarily for simplicity. By adding the kinetic energy of the fluid to the total energy E and constitutive relation, our model could be used to study the active rheology of soft matter [60].

Acknowledgments

This work was partially supported by the National Natural Science Foundation of China no. 12071190, 12231004, and Natural Sciences and Engineering Research Council of Canada (NSERC). S. Xu thanks Prof. Kai Zhang and Prof. Changcheng Zheng for suggestions and helpful discussions.

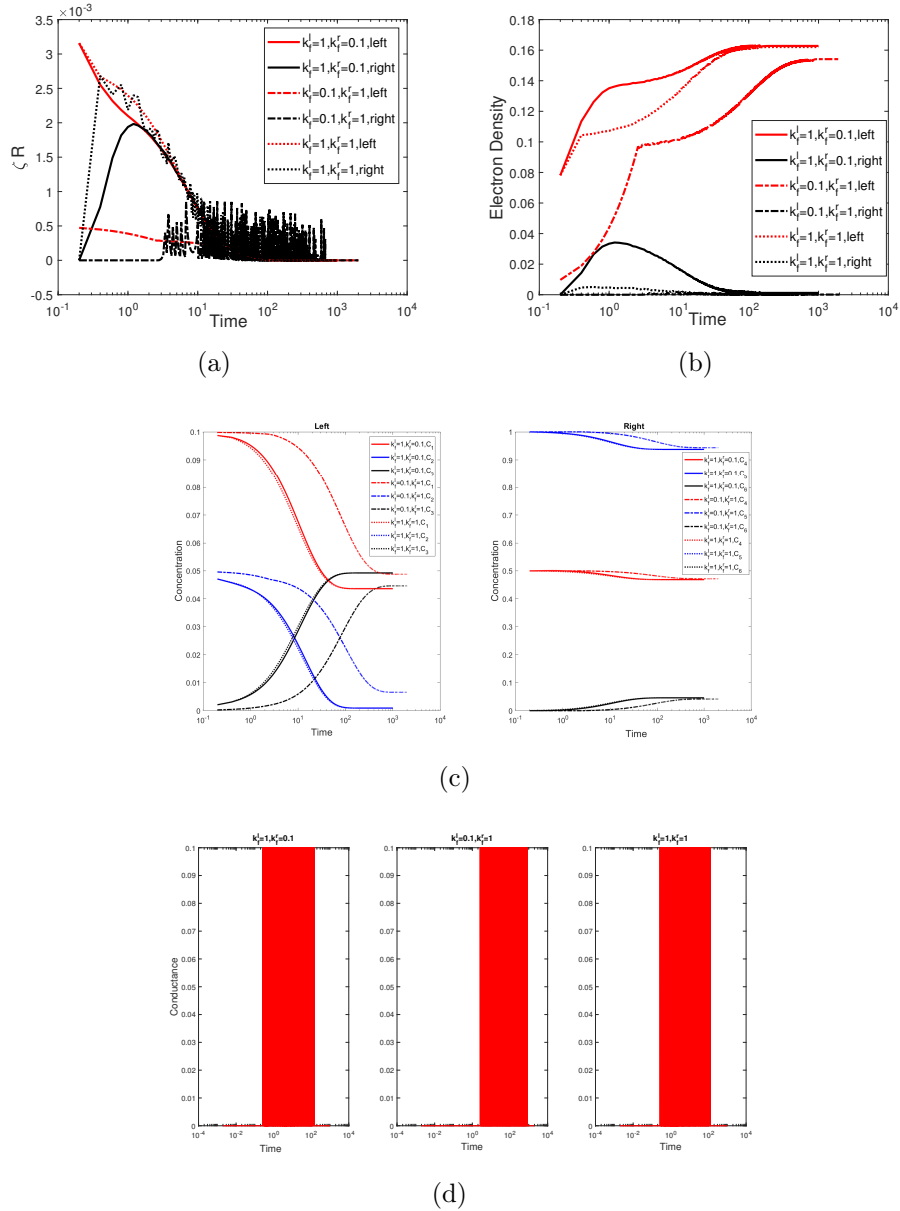


Figure 9: Dynamics evolution of (a) Reaction rates; (b) Electron Density; (c) Substance concentrations; (d) Conductance function over time with different intrinsic reaction rates on both sides of the plate. Here we fix the effective capacitance $\lambda_s = 0.1$ and diffusion-reaction time scale ratio $\zeta = 1$. Hard switch function is used. Dimensional units are used as defined in the beginning of the Results Section.

References

- [1] Martin Z Bazant. Theory of electrochemical kinetics based on nonequilibrium thermodynamics, 2012.
- [2] Martin Z Bazant. Theory of chemical kinetics and charge transfer based on nonequilibrium thermodynamics. *Accounts of chemical research*, 46(5):1144–1160, 2013.
- [3] Martin Z Bazant, Kevin T Chu, and Bruce J Bayly. Current-voltage relations for electrochemical thin films. *SIAM journal on applied mathematics*, 65(5):1463–1484, 2005.
- [4] Ilya Belevich, Dmitry A Bloch, Nikolai Belevich, Mårten Wikström, and Michael I Verkhovsky. Exploring the proton pump mechanism of cytochrome c oxidase in real time. *Proceedings of the*

- National Academy of Sciences*, 104(8):2685–2690, 2007.
- [5] Francisco Bezanilla. The action potential: from voltage-gated conductances to molecular structures. *Biological research*, 39(3):425–435, 2006.
- [6] PM Biesheuvel, Michiel Van Soestbergen, and Martin Z Bazant. Imposed currents in galvanic cells. *Electrochimica Acta*, 54(21):4857–4871, 2009.
- [7] Dmitry Bloch, Ilya Belevich, Audrius Jasaitis, Camilla Ribacka, Anne Puustinen, Michael I Verkhovskiy, and Mårten Wikström. The catalytic cycle of cytochrome c oxidase is not the sum of its two halves. *Proceedings of the National Academy of Sciences*, 101(2):529–533, 2004.
- [8] Margareta RA Blomberg and Per EM Siegbahn. The mechanism for proton pumping in cytochrome c oxidase from an electrostatic and quantum chemical perspective. *Biochimica et Biophysica Acta (BBA)-Bioenergetics*, 1817(4):495–505, 2012.
- [9] Antoine Bonnefont, Françoise Argoul, and Martin Z Bazant. Analysis of diffuse-layer effects on time-dependent interfacial kinetics. *Journal of Electroanalytical Chemistry*, 500(1-2):52–61, 2001.
- [10] Edouard Brunet and Armand Ajdari. Generalized onsager relations for electrokinetic effects in anisotropic and heterogeneous geometries. *Physical Review E*, 69(1):016306, 2004.
- [11] Stephen G Brush. *The kind of motion we call heat*, volume 2. North-Holland Amsterdam, 1976.
- [12] J A_ V Butler. Studies in heterogeneous equilibria. part ii.—the kinetic interpretation of the nernst theory of electromotive force. *Transactions of the Faraday Society*, 19(March):729–733, 1924.
- [13] Xiuhong Cai, Kamran Haider, Jianxun Lu, Slaven Radic, Chang Yun Son, Qiang Cui, and MR Gunner. Network analysis of a proposed exit pathway for protons to the p-side of cytochrome c oxidase. *Biochimica et Biophysica Acta (BBA)-Bioenergetics*, 1859(10):997–1005, 2018.
- [14] William A Catterall. From ionic currents to molecular mechanisms: the structure and function of voltage-gated sodium channels. *Neuron*, 26(1):13–25, 2000.
- [15] C Chree. The mathematical theory of electricity and magnetism. *Nature*, 78(2031):537–538, 1908.
- [16] Kevin C de Berg and Kevin C de Berg. The reaction: Chemical affinity: Laws, theories and models. *The Iron (III) Thiocyanate Reaction: Research History and Role in Chemical Analysis*, pages 41–52, 2019.
- [17] Antoine-Laurent de Lavoisier. *Traité élémentaire de chimie*. Maxtor France, 2019.
- [18] Edmund JF Dickinson and Andrew J Wain. The butler-volmer equation in electrochemical theory: Origins, value, and practical application. *Journal of Electroanalytical Chemistry*, 872:114145, 2020.
- [19] Masao Doi. Variational principle for the kirkwood theory for the dynamics of polymer solutions and suspensions. *The Journal of chemical physics*, 79(10):5080–5087, 1983.
- [20] SF Edwards and Karl F Freed. Theory of the dynamical viscosity of polymer solutions. *The Journal of Chemical Physics*, 61(3):1189–1202, 1974.
- [21] Bob Eisenberg, Yunkyong Hyon, and Chun Liu. Energy variational analysis of ions in water and channels: Field theory for primitive models of complex ionic fluids. *The Journal of Chemical Physics*, 133(10):104104, 2010.
- [22] Tibor Erdey-Grúz and Max Volmer. Zur theorie der wasserstoff überspannung. *Zeitschrift für physikalische Chemie*, 150(1):203–213, 1930.
- [23] RP0138 Feynman, RB Leighton, and ML Sands. Feynman lectures on physics, vol. 2, lecture 19, 2006.

- [24] Bruce A Finlayson. Existence of variational principles for the navier-stokes equation. *The physics of fluids*, 15(6):963–967, 1972.
- [25] Dimitrios Fraggedakis, Michael McEldrew, Raymond B Smith, Yamini Krishnan, Yirui Zhang, Peng Bai, William C Chueh, Yang Shao-Horn, and Martin Z Bazant. Theory of coupled ion-electron transfer kinetics. *Electrochimica Acta*, 367:137432, 2021.
- [26] David C Gadsby. Ion channels versus ion pumps: the principal difference, in principle. *Nature reviews Molecular cell biology*, 10(5):344–352, 2009.
- [27] Elizabeth Garber, Stephen G Brush, and CWF Everitt. *Maxwell on Heat and Statistical Mechanics: On "Avoiding All Personal Enquiries" of Molecules*. Lehigh University Press, 1995.
- [28] Hao Ge and Hong Qian. Mesoscopic kinetic basis of macroscopic chemical thermodynamics: A mathematical theory. *Physical Review E*, 94(5):052150, 2016.
- [29] Pierre-Gilles Gennes, Françoise Brochard-Wyart, David Quéré, et al. *Capillarity and wetting phenomena: drops, bubbles, pearls, waves*. Springer, 2004.
- [30] Runyu Guo, Jinke Gu, Shuai Zong, Meng Wu, and Maojun Yang. Structure and mechanism of mitochondrial electron transport chain. *Biomedical journal*, 41(1):9–20, 2018.
- [31] AL im HODGKIN. Ionic currents underlying activity in the giant axon of the squid. *Arch. Sci. Physiol.*, 3:129–150, 1949.
- [32] Alan L Hodgkin and Andrew F Huxley. A quantitative description of membrane current and its application to conduction and excitation in nerve. *The Journal of physiology*, 117(4):500, 1952.
- [33] Alan L Hodgkin, Andrew F Huxley, and Bernard Katz. Measurement of current-voltage relations in the membrane of the giant axon of loligo. *The Journal of physiology*, 116(4):424, 1952.
- [34] Patrik Knopf, Kei Fong Lam, Chun Liu, and Stefan Metzger. Phase-field dynamics with transfer of materials: the cahn–hilliard equation with reaction rate dependent dynamic boundary conditions. *ESAIM: Mathematical Modelling and Numerical Analysis*, 55(1):229–282, 2021.
- [35] Chun Liu, Tiezheng Qian, and Xinpeng Xu. Hydrodynamic boundary conditions for one-component liquid-gas flows on non-isothermal solid substrates. *Communications in Mathematical Sciences*, 10(4):1027–1053, 2012.
- [36] Chun Liu, Cheng Wang, and Yiwei Wang. A structure-preserving, operator splitting scheme for reaction-diffusion equations with detailed balance. *Journal of Computational Physics*, 436:110253, 2021.
- [37] Chun Liu and Hao Wu. An energetic variational approach for the cahn–hilliard equation with dynamic boundary condition: model derivation and mathematical analysis. *Archive for Rational Mechanics and Analysis*, 233(1):167–247, 2019.
- [38] Alexander Mielke, Robert IA Patterson, Mark A Peletier, and DR3691731 Michiel Renger. Non-equilibrium thermodynamical principles for chemical reactions with mass-action kinetics. *SIAM Journal on Applied Mathematics*, 77(4):1562–1585, 2017.
- [39] AA Moya, J Castilla, and J Horno. Ionic transport in electrochemical cells including electrical double-layer effects. a network thermodynamics approach. *The Journal of Physical Chemistry*, 99(4):1292–1298, 1995.
- [40] WD Murphy, JA Manzanares, S Mafé, and H Reiss. A numerical study of the equilibrium and nonequilibrium diffuse double layer in electrochemical cells. *The Journal of Physical Chemistry*, 96(24):9983–9991, 1992.

- [41] David L Nelson, Albert L Lehninger, and Michael M Cox. *Lehninger principles of biochemistry*. Macmillan, 2008.
- [42] Madeline Nieves-Cintrón, Arsalan U Syed, Matthew A Nystoriak, and Manuel F Navedo. Regulation of voltage-gated potassium channels in vascular smooth muscle during hypertension and metabolic disorders. *Microcirculation*, 25(1):e12423, 2018.
- [43] Lars Onsager. Reciprocal relations in irreversible processes. i. *Physical review*, 37(4):405, 1931.
- [44] Lars Onsager. Reciprocal relations in irreversible processes. ii. *Physical review*, 38(12):2265, 1931.
- [45] Muzaffer ozcan. Why equilibrium constants are unitless. *The Journal of Physical Chemistry Letters*, 13(15):3507–3509, 2022.
- [46] Tiezheng Qian, Xiao-Ping Wang, and Ping Sheng. A variational approach to moving contact line hydrodynamics. *Journal of Fluid Mechanics*, 564:333–360, 2006.
- [47] Weiqing Ren, Dan Hu, and Weinan E. Continuum models for the contact line problem. *Physics of fluids*, 22(10):102103, 2010.
- [48] Rolf Josef Ryham. An energetic variational approach to mathematical modeling of charged fluids: charge phases, simulation and well posedness. 2006.
- [49] Ken Sekimoto. *Stochastic energetics*, volume 799. Springer, 2010.
- [50] Lingyue Shen, Huaxiong Huang, Ping Lin, Zilong Song, and Shixin Xu. An energy stable c_0 finite element scheme for a quasi-incompressible phase-field model of moving contact line with variable density. *Journal of Computational Physics*, 405:109179, 2020.
- [51] Lingyue Shen, Zhiliang Xu, Ping Lin, Huaxiong Huang, and Shixin Xu. An energy stable c^0 finite element scheme for a phase-field model of vesicle motion and deformation. *SIAM Journal on Scientific Computing*, 44(1):B122–B145, 2022.
- [52] Thomas K Simpson. Maxwell on the electromagnetic field: A guided study., 1998.
- [53] Stephanie A Smith, Richard J Travers, and James H Morrissey. How it all starts: Initiation of the clotting cascade. *Critical reviews in biochemistry and molecular biology*, 50(4):326–336, 2015.
- [54] JW Strutt. Some general theorems relating to vibrations. *Proceedings of the London Mathematical Society*, 1(1):357–368, 1871.
- [55] Clifford Truesdell. *Rational thermodynamics: a course of lectures on selected topics*. McGraw-Hill, 1969.
- [56] M Van Soestbergen, PM Biesheuvel, and Martin Z Bazant. Diffuse-charge effects on the transient response of electrochemical cells. *Physical Review E*, 81(2):021503, 2010.
- [57] Michiel Van Soestbergen. Frumkin-butler-volmer theory and mass transfer in electrochemical cells. *Russian journal of electrochemistry*, 48(6):570–579, 2012.
- [58] Marina L Verkhovskaya, Nikolai Belevich, Liliya Euro, Märten Wikström, and Michael I Verkhovsky. Real-time electron transfer in respiratory complex i. *Proceedings of the National Academy of Sciences*, 105(10):3763–3767, 2008.
- [59] Michael I Verkhovsky, Ilya Belevich, Dmitry A Bloch, and Märten Wikström. Elementary steps of proton translocation in the catalytic cycle of cytochrome oxidase. *Biochimica et Biophysica Acta (BBA)-Bioenergetics*, 1757(5-6):401–407, 2006.
- [60] Haiqin Wang, Tiezheng Qian, and Xinpeng Xu. Onsager’s variational principle in active soft matter. *Soft Matter*, 17(13):3634–3653, 2021.

- [61] Qi Wang. Generalized onsager principle and it applications. *Frontiers and Progress of Current Soft Matter Research*, pages 101–132, 2021.
- [62] Yiwei Wang and Chun Liu. Some recent advances in energetic variational approaches. *Entropy*, 24(5):721, 2022.
- [63] Yiwei Wang, Chun Liu, Pei Liu, and Bob Eisenberg. Field theory of reaction-diffusion: Law of mass action with an energetic variational approach. *Physical Review E*, 102(6):062147, 2020.
- [64] Mårten Wikström and Vivek Sharma. Proton pumping by cytochrome c oxidase—a 40 year anniversary. *Biochimica et Biophysica Acta (BBA)-Bioenergetics*, 1859(9):692–698, 2018.
- [65] Mårten Wikström, Michael I Verkhovsky, and Gerhard Hummer. Water-gated mechanism of proton translocation by cytochrome c oxidase. *Biochimica et Biophysica Acta (BBA)-Bioenergetics*, 1604(2):61–65, 2003.
- [66] Shixin Xu, Xinfu Chen, Chun Liu, and Xingye Yue. Numerical method for multi-alleles genetic drift problem. *SIAM Journal on Numerical Analysis*, 57(4):1770–1788, 2019.
- [67] Shixin Xu, Ping Sheng, and Chun Liu. An energetic variational approach for ion transport. *arXiv preprint arXiv:1408.4114*, 2014.
- [68] Xinpeng Xu and Tiezheng Qian. Generalized lorentz reciprocal theorem in complex fluids and in non-isothermal systems. *Journal of Physics: Condensed Matter*, 31(47):475101, 2019.
- [69] Zhiliang Xu, Joshua Lioi, Jian Mu, Malgorzata M Kamocka, Xiaomin Liu, Danny Z Chen, Elliot D Rosen, and Mark Alber. A multiscale model of venous thrombus formation with surface-mediated control of blood coagulation cascade. *Biophysical journal*, 98(9):1723–1732, 2010.
- [70] David Yan, Mary C Pugh, and Francis P Dawson. Adaptive time-stepping schemes for the solution of the poisson-nernst-planck equations. *Applied Numerical Mathematics*, 163:254–269, 2021.
- [71] Xiaogang Yang, Jun Li, M Gregory Forest, and Qi Wang. Hydrodynamic theories for flows of active liquid crystals and the generalized onsager principle. *Entropy*, 18(6):202, 2016.
- [72] Wen-An Yong. Conservation-dissipation structure of chemical reaction systems. *Physical Review E*, 86(6):067101, 2012.
- [73] Andrew Zangwill. *Modern electrodynamics*. Cambridge University Press, 2013.
- [74] Zhen Zhang, Shixin Xu, and Weiqing Ren. Derivation of a continuum model and the energy law for moving contact lines with insoluble surfactants. *Physics of Fluids*, 26(6):062103, 2014.
- [75] Quan Zhao, Weiqing Ren, and Zhen Zhang. A thermodynamically consistent model and its conservative numerical approximation for moving contact lines with soluble surfactants. *Computer Methods in Applied Mechanics and Engineering*, 385:114033, 2021.
- [76] Ru-Zhou Zhao, Shuai Jiang, Lin Zhang, and Zhi-Bin Yu. Mitochondrial electron transport chain, ros generation and uncoupling. *International journal of molecular medicine*, 44(1):3–15, 2019.

A Details of derivation

Eq.(11) derivation

$$\begin{aligned}
\frac{dE}{dt} &= \int_{\Omega} \sum_{i=1}^N \left\{ \mu_i \frac{\partial C_i}{\partial t} \right\} dx + \int_{\Omega} \mathbf{E} \cdot \frac{\partial \mathbf{D}}{\partial t} dx \\
&= \int_{\Omega} \sum_{i=1}^N \left\{ \mu_i \frac{\partial C_i}{\partial t} \right\} dx - \int_{\Omega} \nabla \phi \cdot \frac{\partial \mathbf{D}}{\partial t} dx \\
&= \int_{\Omega} \sum_{i=1}^N \left\{ \mu_i \frac{\partial C_i}{\partial t} \right\} dx + \int_{\Omega} \phi \nabla \cdot \left(\frac{\partial \mathbf{D}}{\partial t} \right) dx \\
&= \int_{\Omega} \sum_{i=1}^N \left\{ \mu_i \frac{\partial C_i}{\partial t} \right\} dx + \int_{\Omega} \phi F \sum_{i=1}^N \left\{ z_i \frac{\partial C_i}{\partial t} \right\} dx \\
&= \int_{\Omega} \sum_{i=1}^N \left\{ \tilde{\mu}_i \frac{\partial C_i}{\partial t} \right\} dx \\
&= - \int_{\Omega} \sum_{i=1}^N \{ \tilde{\mu}_i \nabla \cdot \mathbf{j}_i \} dx + \int_{\Omega} \mathcal{R} \sum_{i=1}^N \gamma_i \tilde{\mu}_i dx \\
&= \int_{\Omega} \sum_{i=1}^N \{ \nabla \tilde{\mu}_i \cdot \mathbf{j}_i \} dx + \int_{\Omega} \mathcal{R} \sum_{i=1}^N \gamma_i \tilde{\mu}_i dx - \int_{\partial \Omega} \sum_{i=1}^N (\tilde{\mu}_i - \tilde{\mu}_{i,ex}) \mathbf{j}_i \cdot \mathbf{n} dS - \int_{\partial \Omega} \tilde{\mu}_{i,ex} \mathbf{j}_i \cdot \mathbf{n} dS. \\
&= -\Delta + \mathcal{P}_{E,\partial \Omega}.
\end{aligned}$$

Eq.(29) derivation

$$\begin{aligned}
&\frac{dE}{dt} \\
&= \int_{\Omega} \sum_{i=1}^N \left\{ \tilde{\mu}_i \frac{\partial C_i}{\partial t} \right\} dx - \int_{\partial \Omega} \phi \frac{\partial \mathbf{D} \cdot \mathbf{n}}{\partial t} dS + \int_{\Gamma} \mu_e \frac{\partial C_e}{\partial t} dS + \int_{\Gamma} (\phi - \phi_p) F \frac{\partial C_e}{\partial t} dS \\
&= - \int_{\Omega} \sum_{i=1}^N \{ \tilde{\mu}_i \nabla \cdot \mathbf{j}_i \} dx - \int_{\partial \Omega} \phi \frac{\partial \mathbf{D} \cdot \mathbf{n}}{\partial t} dS + \int_{\Gamma} \tilde{\mu}_e \frac{\partial C_e}{\partial t} dS + \int_{\Gamma} \phi F \frac{\partial C_e}{\partial t} dS \\
&= - \int_{\Omega} \sum_{i=1}^N \{ \tilde{\mu}_i \nabla \cdot \mathbf{j}_i \} dx - \int_{\Gamma} \phi \frac{\partial}{\partial t} (\mathbf{D} \cdot \mathbf{n} - FC_e) dS + \int_{\Gamma} \tilde{\mu}_e (j_{ex} - \Delta z \mathcal{R}) dS \\
&\quad - \int_{\partial \Omega / \Gamma} \phi \frac{\partial \mathbf{D} \cdot \mathbf{n}}{\partial t} dS \\
&= \int_{\Omega} \sum_{i=1}^N \{ \nabla \tilde{\mu}_i \cdot \mathbf{j}_i \} dx - \int_{\Gamma} \phi \frac{\partial}{\partial t} (\mathbf{D} \cdot \mathbf{n} - FC_e) dS - \int_{\Gamma} \sum_i \tilde{\mu}_i \mathbf{j}_i \cdot \mathbf{n} dS + \int_{\Gamma} \tilde{\mu}_e (-\Delta z \mathcal{R}) dS \\
&\quad - \int_{\partial \Omega / \Gamma} \phi \frac{\partial \mathbf{D} \cdot \mathbf{n}}{\partial t} dS - \int_{\partial \Omega / \Gamma} \sum_i \tilde{\mu}_i \mathbf{j}_i \cdot \mathbf{n} dS + \int_{\Gamma} \tilde{\mu}_e j_{ex} dS \\
&= \int_{\Omega} \sum_{i=1}^N \{ \nabla \tilde{\mu}_i \cdot \mathbf{j}_i \} dx - \int_{\Gamma} \phi \frac{\partial}{\partial t} (\mathbf{D} \cdot \mathbf{n} - FC_e) dS + \int_{\Gamma} \sum_i \tilde{\mu}_i \gamma_i \mathcal{R} dS - \int_{\Gamma} \tilde{\mu}_e (\Delta z \mathcal{R}) dS \\
&\quad - \int_{\partial \Omega / \Gamma} \phi \frac{\partial \mathbf{D} \cdot \mathbf{n}}{\partial t} dS - \int_{\partial \Omega / \Gamma} \sum_i \tilde{\mu}_i \mathbf{j}_i \cdot \mathbf{n} dS + \int_{\Gamma} (\tilde{\mu}_e - \tilde{\mu}_{ex}) j_{ex} dS + \int_{\Gamma} \tilde{\mu}_{ex} j_{ex} dS \\
&= \int_{\Omega} \sum_{i=1}^N \{ \nabla \tilde{\mu}_i \cdot \mathbf{j}_i \} dx - \int_{\Gamma} \left(- \sum_i \tilde{\mu}_i \gamma_i + \tilde{\mu}_e \Delta z \right) \mathcal{R} dS - \int_{\Gamma} \phi \frac{\partial}{\partial t} (\mathbf{D} \cdot \mathbf{n} - FC_e) dS
\end{aligned}$$

$$\begin{aligned}
& + \int_{\Gamma} (\tilde{\mu}_e - \tilde{\mu}_{ex}) j_{ex} dS + \int_{\Gamma} \tilde{\mu}_{ex} J_{ex} dS - \int_{\partial\Omega/\Gamma} \phi \frac{\partial \mathbf{D} \cdot \mathbf{n}}{\partial t} dS - \int_{\partial\Omega/\Gamma} \sum_i^N \tilde{\mu}_i \mathbf{j}_i \cdot \mathbf{n} dS \\
& = -\Delta + P_{E,\partial\Omega}.
\end{aligned}$$

Eq. (48) derivation

$$\begin{aligned}
& \frac{dE}{dt} - \mathcal{P}_{E,\partial\Omega} \\
& = \frac{dE_l}{dt} + \frac{dE_r}{dt} + \frac{dE_{\Gamma}}{dt} - \int_{\partial\Omega} \phi_{ref} \frac{\partial \mathbf{D} \cdot \mathbf{n}}{\partial t} dx \\
& = \int_{\Omega_l} \sum_{i=1}^N \nabla \tilde{\mu}_i^l \cdot \mathbf{j}_i^l dx - \int_{\Gamma} \sum_{i=1}^N \tilde{\mu}_i^l \mathbf{j}_i^l \cdot \mathbf{n}^l dS - \int_{\Gamma} \phi_l \frac{\partial}{\partial t} (\mathbf{D}^l \cdot \mathbf{n}^l - FC_e^l) dS + \int_{\Gamma} \tilde{\mu}_e^l (-\Delta z^l \mathcal{R}_l - J_e) \\
& \quad \int_{\Omega_r} \sum_{i=1}^N \nabla \tilde{\mu}_i^r \cdot \mathbf{j}_i^r dx - \int_{\Gamma} \sum_{i=1}^N \tilde{\mu}_i^r \mathbf{j}_i^r \cdot \mathbf{n}^r dS - \int_{\Gamma} \phi_r \frac{\partial}{\partial t} (\mathbf{D}^r \cdot \mathbf{n}^r - FC_e^r) dS + \int_{\Gamma} \tilde{\mu}_e^r (-\Delta z^l \mathcal{R}_r + J_e) \\
& \quad - \int_{\partial\Omega} (\phi - \phi_{ref}) \frac{\partial \mathbf{D} \cdot \mathbf{n}}{\partial t} dS \\
& = \int_{\Omega_l} \sum_{i=1}^N \nabla \tilde{\mu}_i^l \cdot \mathbf{j}_i^l dx + \int_{\Gamma} \sum_{i=1}^N \tilde{\mu}_i^l \gamma_i \mathcal{R}^l dS - \int_{\Gamma} \phi_l \frac{\partial}{\partial t} (\mathbf{D}^l \cdot \mathbf{n}^l - FC_e^l) dS + \int_{\Gamma} \tilde{\mu}_e^l (-\Delta z^l \mathcal{R}_l - J_e) \\
& \quad \int_{\Omega_r} \sum_{i=1}^N \nabla \tilde{\mu}_i^r \cdot \mathbf{j}_i^r dx + \int_{\Gamma} \sum_{i=1}^N \tilde{\mu}_i^r \gamma_i \mathcal{R}^r dS - \int_{\Gamma} \phi_r \frac{\partial}{\partial t} (\mathbf{D}^r \cdot \mathbf{n}^r - FC_e^r) dS + \int_{\Gamma} \tilde{\mu}_e^r (-\Delta z^l \mathcal{R}_r + J_e) \\
& \quad - \int_{\partial\Omega} (\phi - \phi_{ref}) \frac{\partial \mathbf{D} \cdot \mathbf{n}}{\partial t} dS \\
& = \int_{\Omega_l} \sum_{i=1}^N \nabla \tilde{\mu}_i^l \cdot \mathbf{j}_i^l dx - \int_{\Gamma} \left(-\sum_{i=1}^N \tilde{\mu}_i^l \gamma_i \mathcal{R}^l + \tilde{\mu}_e^l \Delta z^l \right) \mathcal{R}_l dS - \int_{\Gamma} \phi_l \frac{\partial}{\partial t} (\mathbf{D}^l \cdot \mathbf{n}^l - FC_e^l) dS \\
& \quad + \int_{\Omega_r} \sum_{i=1}^N \nabla \tilde{\mu}_i^r \cdot \mathbf{j}_i^r dx - \int_{\Gamma} \left(-\sum_{i=1}^N \tilde{\mu}_i^r \gamma_i + \Delta z^r \tilde{\mu}_e^r \right) \mathcal{R}^r dS - \int_{\Gamma} \phi_r \frac{\partial}{\partial t} (\mathbf{D}^r \cdot \mathbf{n}^r - FC_e^r) dS \\
& \quad + \int_{\Gamma} (\tilde{\mu}_e^r - \tilde{\mu}_e^l) J_e - \int_{\partial\Omega} (\phi - \phi_{ref}) \frac{\partial \mathbf{D} \cdot \mathbf{n}}{\partial t} dS \\
& = -\Delta.
\end{aligned} \tag{55}$$

B Numerical Scheme

Here we present the detailed numerical scheme for the bidomain reaction system (53)-(54).

$$\begin{cases} \frac{(C_i^s)^{n+1} - (C_i^s)^n}{\Delta t} = \nabla \cdot (D_i^s (\nabla (C_i^s)^{n+1} + z_i (C_i^s)^{n+1} \nabla (\phi^s)^n), \\ -\nabla \cdot (\delta^2 \nabla (\phi^s)^{n+1}) = \sum_{i=1}^N z_i (C_i^s)^{n+1}, \end{cases} \tag{56}$$

with the boundary conditions

$$\begin{cases} (\mathbf{j}_i^s)^{n+1} \cdot \mathbf{n}_s = -\gamma_i \zeta (\mathcal{R}^s)^n, & \text{on } \Gamma, \\ -\nabla (\phi^s)^{n+1} \cdot \mathbf{n}_s = \lambda_s ((\phi^s)^{n+1} - (\phi_p^s)^{n+1}), & \text{on } \Gamma, \\ \lambda_l \frac{((\phi^l)^{n+1} - (\phi_p^l)^{n+1}) - ((\phi^l)^n - (\phi_p^l)^n)}{\Delta t} + \frac{\zeta}{\delta^2} \Delta z_l (\mathcal{R}^l)^n = g \left(\ln \left(\frac{(C_e^r)^{n+1}}{(C_e^l)^{n+1}} \right) + (\phi_p^l)^{n+1} - (\phi_p^r)^{n+1} \right), & \text{on } \Gamma, \\ \lambda_r \frac{((\phi^r)^{n+1} - (\phi_p^r)^{n+1}) - ((\phi^r)^n - (\phi_p^r)^n)}{\Delta t} + \frac{\zeta}{\delta^2} \Delta z_r (\mathcal{R}^r)^n = -g \left(\ln \left(\frac{(C_e^r)^{n+1}}{(C_e^l)^{n+1}} \right) + (\phi_p^l)^{n+1} - (\phi_p^r)^{n+1} \right), & \text{on } \Gamma, \\ (\mathbf{j}^s)^{n+1} \cdot \mathbf{n} = 0, \phi^s = 0, & \text{on } \partial\Omega/\Gamma, \end{cases} \tag{57}$$

where

$$(\mathcal{R}^l)^n = k_{f,0}^l e^{-\Delta Z_l \beta ((\phi_p^l)^n - (\phi^l)^n)} \prod_{i=1}^N \left((C_i^l)^n \right)^{a_i} - k_{r,0}^l e^{\Delta Z_l (1-\beta) ((\phi_p^l)^n - (\phi^l)^n)} \left((C_e^l)^n \right)^{-\Delta z^l} \prod_{i=1}^N \left((C_i^l)^n \right)^{b_i}$$

$$(\mathcal{R}^r)^n = k_{f,0}^r e^{-\Delta Z_r \beta ((\phi_p^r)^n - (\phi^r)^n)} ((C_e^r)^n)^{\Delta z^r} \prod_{i=1}^N ((C_i^r)^n)^{a_i} - k_{r,0}^r e^{\Delta Z_r (1-\beta) ((\phi_p^r)^n - (\phi^r)^n)} \prod_{i=1}^N ((C_i^r)^n)^{b_i}.$$

Finite volume methods [66] are used for space discretization.